4
Differential Flow and Reaction Applications

4.1
Introduction

4.1.1
Dynamic Simulation

The main process variables in differential contacting devices vary continuously with respect to distance. Dynamic simulations therefore involve variations with respect to both time and position. Thus two independent variables, time and position, are now involved. Although the basic principles remain the same, the mathematical formulation for the dynamic system now results in the form of partial differential equations. As most digital simulation languages permit the use of only one independent variable, the second independent variable, either time or distance, is normally eliminated by the use of a finite-differencing procedure. In this chapter, the approach is based very largely on that of Franks (1967), and the distance coordinate is treated by finite differencing.

In this procedure, the length coordinate of the system is divided into N finite-difference elements or segments, each of length ΔZ, where N times ΔZ is equal to the total length or distance. It is assumed that within each element any variation with respect to distance is relatively small. The conditions at the mid-point of the element can therefore be taken to represent the conditions of the element as a whole. This is shown in Fig. 4.1, where the average concentration of any element n is identified by the midpoint concentration C_n. The actual continuous variation in concentration with respect to length is therefore approximated by a series of discontinuous variations.

The dynamic behaviour of element n is affected by the conditions in its neighbouring elements $n-1$ and $n+1$, and each original partial differential equation is approximated by a system of N simultaneous difference differential equations. In practice, the length of each element ΔZ may be kept constant or may be varied from segment to segment. A greater number of elements usually improves the approximation of the profile, but the computational effort required is also greater. The approach is demonstrated in the simulation examples DISRET, DISRE, AXDISP, CHROMDIFF, MEMSEP, HEATEX, DRY, ENZDYN, BEAD, SOIL and LEACH.

Chemical Engineering Dynamics: An Introduction to Modelling and Computer Simulation, Third Edition
J. Ingham, I. J. Dunn, E. Heinzle, J. E. Prenosil, J. B. Snape

ISBN: 978-3-527-31678-6

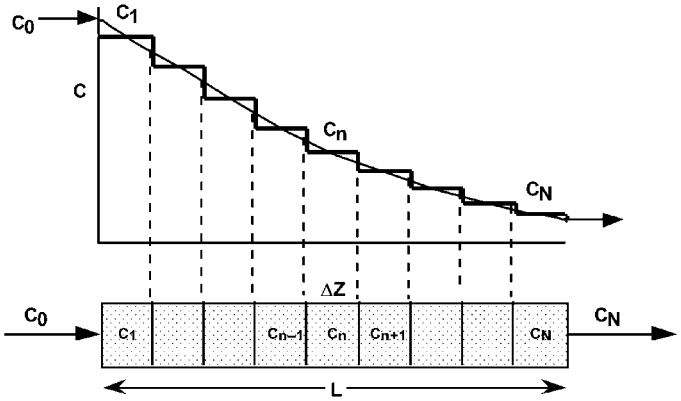

Fig. 4.1 Finite-differencing a tubular reactor with the stepwise approximation of the continuous concentration profile.

4.1.2 Steady-State Simulation

Under steady-state conditions, variations with respect to time are eliminated and the steady-state model can now be formulated in terms of the one remaining independent variable, length or distance. In many cases, the model equations now become simultaneous first-order differential equations, for which solution is straightforward. Simulation examples of this type are the steady-state tubular reactor models TUBE and TUBEDIM, TUBTANK, ANHYD, BENZHYD and NITRO.

Some models, however, take the form of second-order differential equations, which often give rise to problems of the split boundary type. In order to solve this type of problem, an iterative method of solution is required, in which an unknown condition at the starting point is guessed, the differential equation integrated. After comparison with the second boundary condition a new starting point is estimated, followed by re-integration. This procedure is then repeated until convergence is achieved. MADONNA provides such a method. Examples of the steady-state split-boundary type of solution are shown by the simulation examples ROD and ENZSPLIT.

In order to overcome the problem of split boundaries, it is sometimes preferable to formulate the model dynamically, and to obtain the steady-state solution, as a consequence of the dynamic solution, leading to the eventual steady state. This procedure is demonstrated in simulation example ENZDYN.

4.2
Diffusion and Heat Conduction

This section deals with problems involving diffusion and heat conduction. Both diffusion and heat conduction are described by similar forms of equation. Fick's Law for diffusion has already been met in Section 1.2.2 and the similarity of this to Fourier's Law for heat conduction is apparent.

With Fick's Law

$$j_A = -D\frac{dC_A}{dZ}$$

and Fourier's Law

$$q = -k\frac{dT}{dZ}$$

Here j_A is the diffusional flux of component A (kmol/m^2 s), D is the diffusion coefficient (m^2/s), C_A is the concentration of component A (kmol/m^3), q is the heat transfer flux (kJ/m^2 s), k is the thermal conductivity (kJ/m s K), T is the temperature (K) and Z is the distance (m).

In diffusional mass transfer, the transfer is always in the direction of decreasing concentration and is proportional to the magnitude of the concentration gradient, the constant of proportionality being the diffusion coefficient for the system.

In conductive heat transfer, the transfer is always in the direction of decreasing temperature and is proportional to the magnitude of the temperature gradient, the constant of proportionality being the thermal conductivity of the system.

The analogy also extends to Newton's equation for momentum transport, where

$$\tau = -\mu\frac{dv}{dZ}$$

where, for Newtonian liquids, μ is the viscosity, τ is the shear stress, v is velocity and Z is again distance.

4.2.1
Unsteady-State Diffusion through a Porous Solid

This problem illustrates the solution approach to a one-dimensional, non-steady-state, diffusional problem, as demonstrated in the simulation examples, DRY and ENZDYN. The system is represented in Fig. 4.2. Water diffuses through a porous solid, to the surface, where it evaporates into the atmosphere.

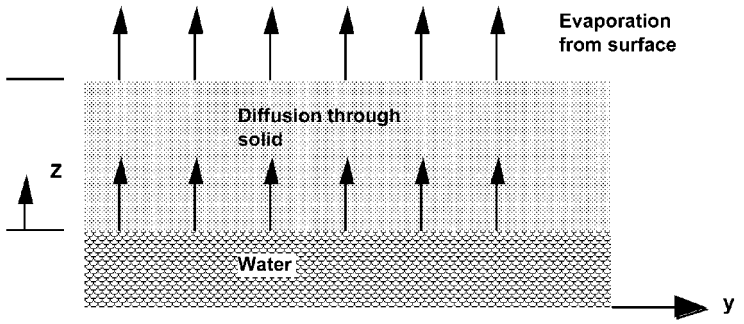

Fig. 4.2 Unsteady-state diffusion through a porous solid.

It is required to determine the water concentration profile in the solid, under drying conditions. The quantity of water is limited and, therefore, the solid will eventually dry out and the drying rate will reduce to zero.

The movement of water through a solid, such as wood, in the absence of chemical reaction, is described by the following time-dependent diffusional equation.

$$\frac{\partial C}{\partial t} = -D\frac{\partial^2 C}{\partial Z^2}$$

where, at steady state, $\partial C/\partial t = 0$, and

$$0 = D\frac{d^2 C}{dZ^2}$$

integrating

$$\frac{dC}{dZ} = \text{constant}$$

Thus at steady state the concentration gradient is constant.

Note that since there are two independent variables of both length and time, the defining equation is written in terms of the partial differentials, $\partial C/\partial t$ and $\partial C/\partial Z$, whereas at steady state only one independent variable, length, is involved and the ordinary derivative function is used. In reality the above diffusion equation results from a combination of an unsteady-state material balance, based on a small differential element of solid length dZ, combined with Fick's Law of diffusion.

To set up the problem for simulation involves discretising one of the independent variables, in this case length, and solving the time-dependent equations, obtained for each element, by means of a simulation language. By finite-differencing the length coordinate of the solid, as shown in Fig. 4.3, the drying process is approximated to that of a series of finite-differenced solid segments.

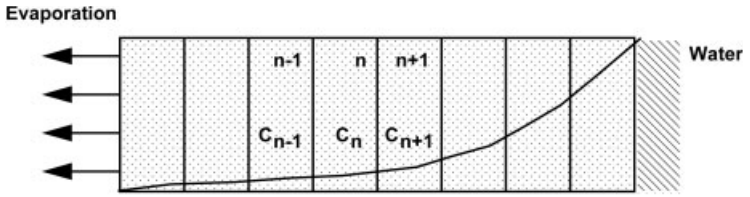

Fig. 4.3 Finite-differenced equivalent of the depth of solid.

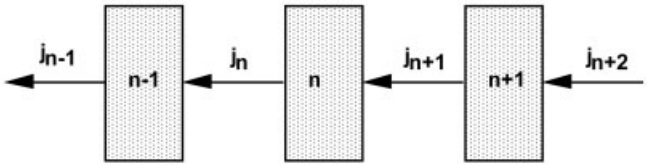

Fig. 4.4 Diffusional fluxes from segment to segment.

The diffusional fluxes from segment to segment are indicated in Fig. 4.4.

Note that the segments are assumed to be so small, that any variation in concentration within the segment, with respect to length, can effectively be ignored. The effective concentration of the segment can therefore be taken as that at the midpoint.

A component material balance is written for each segment, where

$$\begin{pmatrix}\text{Rate of accumulation}\\ \text{in the segment}\end{pmatrix} = \begin{pmatrix}\text{Diffusional}\\ \text{flow in}\end{pmatrix} - \begin{pmatrix}\text{Diffusional}\\ \text{flow out}\end{pmatrix}$$

or

$$\Delta V_n \frac{dC_n}{dt} = (j_{n+1} - j_n)A$$

Here j_n is the mass flux leaving segment n (kg/m^2 s), C_n is the concentration of segment n (kg/m^3), A is the cross-sectional area (m^2), t is time (t) and ΔV_n is the volume of segment n (m^3).

By Fick's Law
$$j = -D\frac{dC}{dZ}$$

with dimensions
$$\frac{M}{L^2T} = \frac{L^2}{T}\frac{M}{L^3L}$$

The concentration gradient terms, dC/dZ, both in and out of segment n, can be approximated by means of their finite-differenced equivalents. Substituting these into the component balance equation gives

$$\Delta V_n \frac{dC_n}{dt} = D\frac{(C_{n+1} - C_n)}{\Delta Z}A - D\frac{(C_n - C_{n-1})}{\Delta Z}A$$

where ΔZ is the length of the segment and $\Delta V_n = A\,\Delta Z$. Thus

$$\frac{dC_n}{dt} = D\frac{(C_{n+1} - 2C_n + C_{n-1})}{\Delta Z^2}$$

The above procedure is applied to all the finite-difference segments in turn. The end segments ($n=1$ and $n=N$), however, often require special attention according to particular boundary conditions: For example, at $Z=L$ the solid is in contact with pure water and $C_{N+1}=C_{eq,}$ where the equilibrium concentration C_{eq} would be determined by prior experiment.

At the air–solid surface, $Z=0$, the drying rate is determined by the convective heat and mass transfer drying conditions and the surrounding atmosphere of the drier. Assuming that the drying rate is known, the component balance equation for segment 1 becomes

$$\begin{pmatrix}\text{Rate of accumulation}\\ \text{in segment 1}\end{pmatrix} = \begin{pmatrix}\text{Rate of input}\\ \text{by diffusion}\\ \text{from segment 2}\end{pmatrix} - \begin{pmatrix}\text{Rate of}\\ \text{drying}\\ \text{from surface}\end{pmatrix}$$

Alternatively, the concentration in segment 1, C_1, may be taken simply as that in equilibrium with the surrounding air.

The unsteady model, originally formulated in terms of a partial differential equation, is thus transformed into N difference differential equations. As a result of the finite-differencing, a solution can be obtained for the variation with respect to time of the water concentration, for every segment throughout the bed.

The simulation example DRY is based directly on the above treatment, whereas ENZDYN models the case of unsteady-state diffusion combined with chemical reaction. Unsteady-state heat conduction can be treated in an exactly analogous manner, though for cases of complex geometry, with multiple heat sources and sinks, the reader is referred to specialist texts, such as Carslaw and Jaeger (1959).

4.2.2
Unsteady-State Heat Conduction and Diffusion in Spherical and Cylindrical Coordinates

Although the foregoing example in Section 4.2.1 is based on a linear coordinate system, the methods apply equally to other systems, represented by cylindrical and spherical coordinates. An example of diffusion in a spherical coordinate system is provided by simulation example BEAD. Here the only additional complication in the basic modelling approach is the need to describe the geometry

of the system, in terms of the changing area for diffusional flow through the bead.

4.2.3 Steady-State Diffusion with Homogeneous Chemical Reaction

The following example, taken from Welty et al. (1976), illustrates the solution approach to a steady-state, one-dimensional, diffusion or heat conduction problem.

As shown in Fig. 4.5, an inert gas containing a soluble component S stands above the quiescent surface of a liquid, in which the component S is both soluble and in which it reacts chemically to form an inert product. Assuming the concentration of S at the gas–liquid surface to be constant, it is desired to determine the rate of solution of component S and the subsequent steady-state concentration profile within the liquid.

Under quiescent conditions, the rate of solution of S within the liquid is determined by molecular diffusion and is described by Fick's Law, where

$$j_S = -D\frac{dC_S}{dZ} \quad \text{kmol/m}^2\text{s}$$

At steady-state conditions, the rate of supply of S by diffusion is balanced by the rate of consumption by chemical reaction, where assuming a first-order chemical reaction

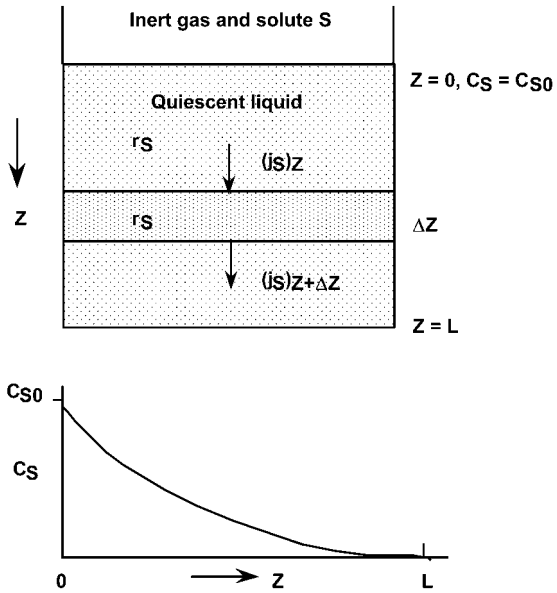

Fig. 4.5 Steady-state diffusion with chemical reaction.

$$r_S = -kC_S$$

with typical units of kmol/m^{3}s.

Thus considering a small differential element of liquid volume, dV, and depth, dZ, the balance equation becomes

$$j_S A_S = r_S dV$$

where A_S is the cross-sectional area of the element and $dV = A_S\,dZ$.

Hence

$$-D\frac{dC_S}{dZ}A_S = -kC_S A_S dZ$$

or

$$-D\frac{d^2C_S}{dZ^2} + kC_S = 0$$

where each term has the dimensions mass/time or units (kmol/s).

The above second-order differential equation can be solved by integration. At the liquid surface, where $Z=0$, the bulk gas concentration, C_{S0}, is known, but the concentration gradient dC_S/dZ is unknown. Conversely at the full liquid depth, the concentration C_{S0} is not known, but the concentration gradient is known and is equal to zero. Since there can be no diffusion of component S from the bottom surface of the liquid, i.e., j_S at $Z=L$ is 0 and hence from Fick's Law dC_S/dZ at $Z=L$ must also be zero.

The problem is thus one of a split boundary value type, and it can be solved by an iterative procedure based on an assumed value for one of the unknown boundary conditions. Assuming a value for dC_S/dZ at the initial condition $Z=0$, the equation can be integrated twice to produce values of dC_S/dZ and C_S at the terminal condition, $Z=L$. If the correct initial value has been chosen, the integration will lead to the correct final boundary condition, i.e., that $dC_S/dZ=0$ at $Z=L$ and hence give the correct values of C_S. The value of the concentration gradient dC_S/dZ is also obtained for all values of Z throughout the depth of liquid.

Further applications of this method are given in the simulation examples ENZSPLIT and ROD.

4.3 Tubular Chemical Reactors

Mathematical models of tubular chemical reactor behaviour can be used to predict the dynamic variations in concentration, temperature and flow rate at various locations within the reactor. A complete tubular reactor model would however be extremely complex, involving variations in both radial and axial posi-

tions, as well as perhaps spatial variations within individual catalyst pellets. Models of such complexity are beyond the scope of this text, and variations only with respect to both time and axial position are treated here. Allowance for axial dispersion is however included, owing to its very large influence on reactor performance, and the fact that the modelling procedure using digital simulation is relatively straightforward.

4.3.1
The Plug-Flow Tubular Reactor

Consider a small element of volume, ΔV, of an ideal plug-flow tubular reactor, as shown in Fig. 4.6.

Component Balance Equation

A component balance equation can be derived for the element ΔV, based on the generalised component balance expression, where, for any reactant A

$$\begin{pmatrix}\text{Rate of}\\ \text{accumulation}\\ \text{of A}\end{pmatrix} = \begin{pmatrix}\text{Mass}\\ \text{flow}\\ \text{of A in}\end{pmatrix} - \begin{pmatrix}\text{Mass}\\ \text{flow}\\ \text{of A out}\end{pmatrix} + \begin{pmatrix}\text{Rate of}\\ \text{formation}\\ \text{of A by reaction}\end{pmatrix}$$

The rate of accumulation of component A in element ΔV is $(\Delta V\, dC_A/dt)$, where dC_A/dt is the rate of change of concentration.

The mass rate of flow of A into element ΔV is $F\, C_A$, and the rate of flow of A from element ΔV is $F\, C_A + \Delta(F\, C_A)$, where F is the volumetric flow rate. The rate of formation of A by reaction is $r_A \Delta V$, where r_A is the rate per unit volume.

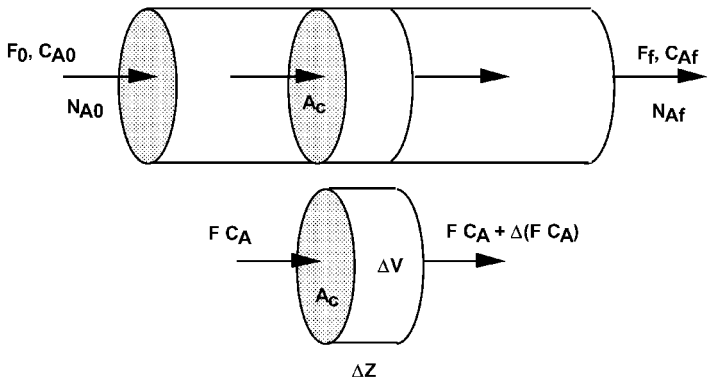

Fig. 4.6 Component balancing for a tubular plug-flow reactor.

Substituting these quantities gives the resulting component balance equation as

$$\Delta V \frac{dC_A}{dt} = F\,C_A - [F\,C_A + \Delta(F\,C_A)] + r_A \Delta V$$

or

$$\frac{dC_A}{dt} = -\frac{\Delta(FC_A)}{\Delta V} + r_A$$

The above equation may also be expressed in terms of length, since

$$\Delta V = A_c \Delta Z$$

where A_c is the cross-sectional area of the reactor.

Allowing ΔV to become very small, the above balance equation is transformed into the following partial differential equation, where

$$\frac{\partial C_A}{\partial t} = -\frac{1}{A_c}\frac{\partial(FC_A)}{\partial Z} + r_A$$

For constant volumetric flow rate, F, throughout the reactor

$$\frac{\partial C_A}{\partial t} = -\frac{F}{A_c}\frac{\partial C_A}{\partial Z} + r_A$$

where F/A_c is the superficial linear fluid velocity v, through the reactor.

Under steady-state conditions

$$\frac{\partial C_A}{\partial t} = 0$$

and hence, at steady state

$$\frac{dC_A}{dZ} = \frac{1}{v} r_A$$

This equation can be integrated to determine the resulting steady-state variation of C_A with respect to Z, knowing the reaction kinetics $r_A = f(C_A)$ and the initial conditions C_A at $Z = 0$.

Cases with more complex multicomponent kinetics will require similar balance equations for all the components of interest.

The component balance equation can also be written in terms of fractional conversion, X_A, where for constant volumetric flow conditions

$$C_A = C_{A0}\,(1 - X_A)$$

and C_{A0} is the inlet reactor feed concentration. Thus

$$dC_A = -C_{A0} dX_A$$

The material balance, in terms of X_A, is thus given by

$$C_{A0}\frac{dX_A}{dZ} = -\frac{1}{v}r_A$$

Reactant A is consumed, so r_A is negative, and the fractional conversion will increase with Z.

In terms of molar flow rates

$$N_{A0}\frac{dX_A}{dZ} = -A_c\, r_A$$

and

$$N_{A0}\frac{dX_A}{dV} = -r_A$$

where N_{A0} is the molar flow of reactant A entering to the reactor.

Energy Balance Equation

The energy balance for element ΔV of the reactor again follows the generalised form, derived in Section 1.2.5. Thus

$$\begin{pmatrix}\text{Rate of}\\ \text{accumulation}\\ \text{of energy}\end{pmatrix} = \begin{pmatrix}\text{Rate of energy}\\ \text{required to}\\ \text{heat the incoming}\\ \text{stream from}\\ \text{T to T} + \Delta\text{T}\end{pmatrix} + \begin{pmatrix}\text{Rate of}\\ \text{energy}\\ \text{generated}\\ \text{by reaction}\\ \text{at T} + \Delta\text{T}\end{pmatrix} - \begin{pmatrix}\text{Rate of}\\ \text{energy}\\ \text{out by}\\ \text{transfer}\end{pmatrix}$$

Referring to Fig. 4.7, the general energy balance for segment n with S components and R reactions is

$$\sum_{i=1}^{S}(n_{in}c_{pin})\frac{dT_n}{dt} = -\sum_{i=1}^{S}N_{in-1}\int_{T_{n-1}}^{T_{n-1}+\Delta T}c_{pin-1}dT + \sum_{j=1}^{R}\frac{R_{ijn}}{\nu_{ij}}(-\Delta H_{jn}) - Q_n$$

With more complex cases, c_p and ΔH are functions of temperature, then the substitutions would be as shown in Case C of Section 1.2.5.3. This general form, which may give rise to very complex expressions, may be important for gas phase reactions (see also Section 4.3.3). Simplifying by assuming only one reaction (R = 1) and constant c_{pi} gives

$$\sum_{i=1}^{S}(n_{in}c_{pin})\frac{dT_n}{dt} = -\sum_{i=1}^{S}(N_{in-1}c_{pin-1}\Delta T_n) + \frac{R_{in}}{\nu_i}(-\Delta H_n) - Q_n$$

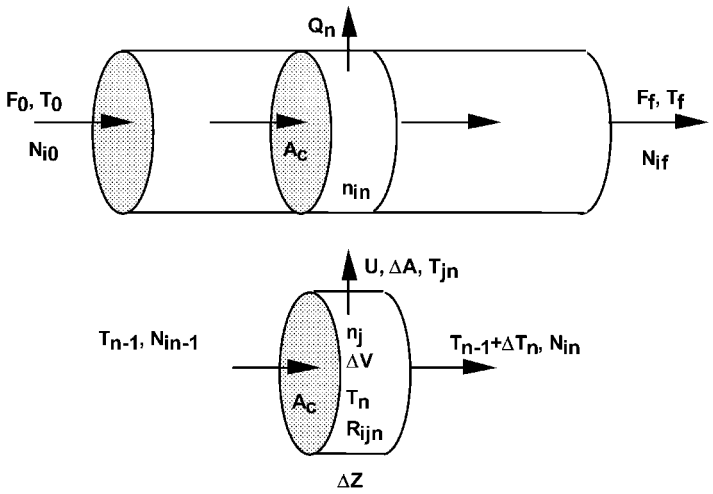

Fig. 4.7 Energy balancing for the tubular plug-flow reactor.

Assuming the total heat capacity to be constant, $\sum_{i=1}^{S}(N_i c_{pi}) = F\rho c_p$, and replacing $\sum_{i=1}^{S}(n_{in} c_{pin})$ by $\Delta V \rho c_p$, the total heat capacity of one element gives

$$\Delta V \rho c_p \frac{dT_n}{dt} = -F \rho c_p \Delta T_n + \Delta V \frac{r_{in}}{\nu_i}(-\Delta H_n) - Q_n$$

The heat loss through the wall to the jacket is

$$Q_n = U\Delta A(T_n - T_j)$$

The term ΔT can be approximated by $(dT/dZ)\Delta Z$ (see also Section 4.3.5). For a tube

$$\frac{\Delta A}{\Delta V} = \frac{d\pi\Delta Z}{\left(\frac{d}{2}\right)^2 \pi\Delta Z} = \frac{4}{d}$$

where d is the tube diameter. Noting further that $\Delta V = A_c \Delta Z$, that the linear velocity $v = F/A_c$ and letting ΔZ approach zero, gives the defining partial differential equation

$$\frac{\partial T}{\partial t} = -v\frac{\partial T}{\partial Z} + \frac{1}{\rho c_p}\frac{r_i}{\nu_i}(-\Delta H) - \frac{4U}{d\rho c_p}(T - T_j)$$

For steady-state conditions, the above equation reduces to

$$\frac{dT}{dZ} = \frac{1}{v\rho c_p}\frac{r_i}{\nu_i}(-\Delta H) - \frac{4U}{v\rho c_p d}(T - T_j)$$

This equation can be integrated together with the component balances and the reaction kinetic expressions where the kinetics could, for example, be of the form

$$r_i = k_i C_i^n = k_0 e^{-E/RT} C_i^n$$

thus including variation of the rate constant k with respect to temperature.

The component material balance equation, combined with the reactor energy balance equation and the kinetic rate equation, provide the basic model for the ideal plug-flow tubular reactor.

4.3.2
Liquid-Phase Tubular Reactors

Assuming the case of a first-order chemical reaction ($r_A = -kC_A$) and a non-compressible liquid system, the generalised mass and energy balance equations reduce to

$$\frac{dC_A}{dZ} = -\frac{k}{v}C_A$$

and

$$\frac{dT}{dZ} = \frac{(-\Delta H)}{v\rho c_p}k C_A - \frac{4U}{v\rho c_p d}(T - T_j)$$

where v, ρ and c_p are assumed constants and k is given by the Arrhenius equation $k = k_0 e^{-E/RT}$.

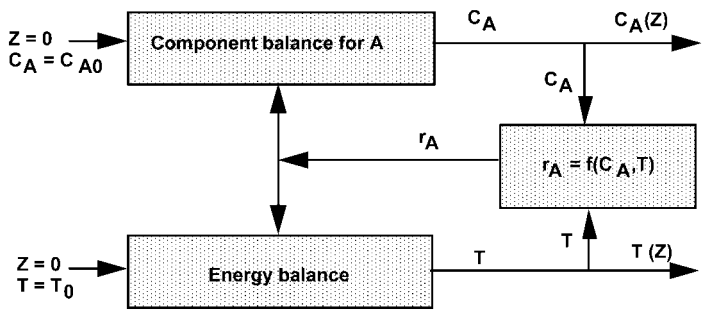

Fig. 4.8 Flow diagram for the simultaneous integration of the balances.

The general solution approach, to this type of problem, is illustrated by the information flow diagram, shown in Fig. 4.8. The integration thus starts with the initial values at $Z=0$, and proceeds with the calculation of r_A, along the length of the reactor, using the computer updated values of T and C_A, which are also produced as outputs.

The simultaneous integration of the two continuity equations, combined with the chemical kinetic relationships, thus gives the steady-state values of both, C_A and T, as functions of reactor length. The simulation examples BENZHYD, ANHYD and NITRO illustrate the above method of solution.

4.3.3 Gas-Phase Tubular Reactors

In gas-phase reactors, the volume and volumetric flow rate frequently vary, owing to the molar changes caused by reaction and the effects of temperature and pressure on gas phase volume. These influences must be taken into account when formulating the mass and energy balance equations.

The Ideal Gas Law can be applied both to the total moles of gas, n, or to the moles of a given component of the gas mixture n_i, where

$$PV = nRT$$

and

$$p_i V = n_i RT$$

Here P is the total pressure of the system, p_i is the partial pressure of component i, V is the volume of the system, T is temperature and R is the Ideal Gas Constant.

Using Dalton's Law

$$p_i = y_i P$$

the relationship for the concentration C_i, in terms of mole fraction y_i, and total pressure is obtained as

$$C_i = \frac{n_i}{V} = \frac{y_i P}{RT}$$

This can also be expressed in terms of the molar flow rate N_i, and the volumetric flow rate G, where

$$N_i = \frac{y_i P G}{RT}$$

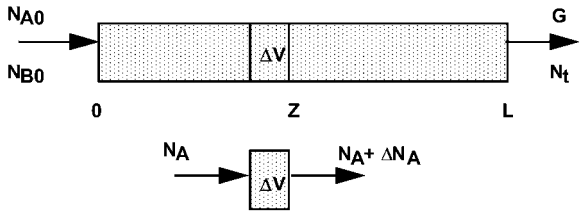

Fig. 4.9 Material balancing for a gas-phase tubular reactor.

Assuming first-order kinetics for the reaction $A \rightarrow m\,B$

$$r_A = -kC_A = -\frac{ky_AP}{RT}$$

and by stoichiometry

$$r_B = mkC_A = \frac{mky_AP}{RT}$$

The steady-state material balance – for a volume element, ΔV, as shown in Fig. 4.9, for reactant A – is given by

$$0 = N_A - (N_A + \Delta N_A) + r_A \Delta V$$

which, since $\Delta V = A_c \Delta Z$, then gives

$$\frac{dN_A}{dZ} = r_A A_c$$

Similarly for component B

$$\frac{dN_B}{dZ} = r_B A_c$$

where A_c is again the cross-sectional flow area of the reactor.

The variation in molar flow can be written as

$$\frac{dN_A}{dZ} = \frac{d\left(\frac{y_APG}{RT}\right)}{dZ}$$

which for constant temperature and pressure conditions becomes

$$\frac{dN_A}{dZ} = \frac{P}{RT}\frac{d(y_AG)}{dZ}$$

Substituting this and the reaction kinetics r_A into the component balance equation for reactant A gives

$$\frac{d(y_A G)}{dZ} = -k y_A A_c \qquad (I)$$

Similarly for B

$$\frac{d(y_B G)}{dZ} = m k y_A A_c \qquad (II)$$

The volumetric flow rate depends on the total molar flow of the gas and the temperature and pressure of reaction, where

$$G = \frac{(N_A + N_B + N_{inerts})RT}{P} \qquad (III)$$

where the molar flow rates of A and B are given by

$$N_A = \frac{y_A G P}{RT} \qquad (IV)$$

and

$$N_B = \frac{y_B G P}{RT} \qquad (V)$$

The model equations, I to V above, provide the basis for solution, for this case of constant temperature and pressure with a molar change owing to chemical reaction. This is illustrated by the information flow diagram (Fig. 4.10). The step-by-step calculation procedure is as follows:

1. The initial molar flow rates of each component at the reactor inlet, $(y_A G)_0$ and $(y_B G)_0$, are known.
2. The component balance equations (I) and (II) are integrated with respect to distance to give the volumetric flow rate of each component, $(y_A G)_Z$ and $(y_B G)_Z$, at any position Z, along the length of the reactor.
3. The total molar flow rate of each component, $(N_A)_Z$ and $(N_B)_Z$, can then be calculated at position Z, from equations (IV) and (V).
4. The total volumetric flow rate G is calculated at each position, using equation (III) and hence:
5. The composition of the gas mixture at position Z is obtained by dividing the individual molar flow rate by the volumetric flow rate.

The results of the calculation are thus the mole fraction compositions y_A and y_B, together with the total volumetric flow rate G, as steady-state functions of reactor length.

The step-by-step evaluation is, of course, effected automatically by the computer, as shown in the simulation example VARMOL.

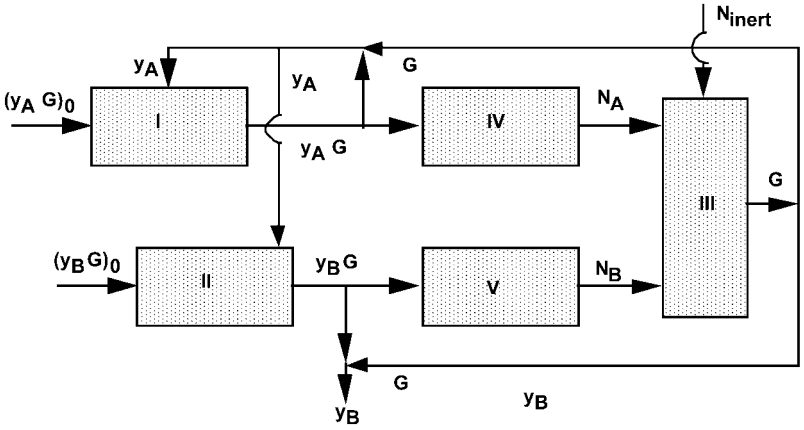

Fig. 4.10 Information flow diagram for a gas-phase tubular reactor with molar change.

To obtain the fractional conversion at any position along the reactor the appropriate equation is

$$N_A = N_{A0}(1 - X_A)$$

where

$$y_A N_{Tot} = y_{A0} N_{Tot0}(1 - X_A)$$

In the case of non-isothermal situations with significant pressure drop through the reactor, the term

$$\frac{d\left(\frac{y_i GP}{RT}\right)}{dZ}$$

must be retained in the model equations. The variation of reactor pressure with reactor length, $(P)_Z$, can be obtained by the use of available pressure drop-flow correlations, appropriate to the reactor geometry and flow conditions. The variation in temperature, with respect to length, $(T)_Z$ must be obtained via a steady-state energy balance equation, as described in Section 4.3.1.

4.3.4
Batch Reactor Analogy

The ideal plug-flow reactor is characterised by the concept that the flow of liquid or gas moves with uniform velocity similar to that of a plug moving through the tube. This means that radial variations of concentration, temperature and flow velocity are neglected and that axial mixing is negligible. Each element of fluid flows through the reactor with the same velocity and therefore remains in the reactor for the same length of time, which is given by the flow volume of the reactor di-

vided by the volumetric flow rate. The residence time of fluid in the ideal tubular reactor is thus analogous to the reaction time in a batch reactor.

With respect to reaction rates, an element of fluid will behave in the ideal tubular reactor, in the same way, as it does in a well-mixed batch reactor. The similarity between the ideal tubular and batch reactors can be understood by comparing the model equations.

For a batch reactor, under constant volume conditions, the component material balance equation can be represented by

$$\frac{dC_A}{dt} = r_A$$

For a plug-flow tubular reactor, the flow velocity v through the reactor can be related to the distance travelled along the reactor or tube Z, and to the time of passage t, where

$$dt = \frac{dZ}{v}$$

Equating the time of passage through the tubular reactor to that of the time required for the batch reaction, gives the equivalent ideal-flow tubular reactor design equation as

$$\frac{dC_A}{dZ} = \frac{r_A}{v}$$

4.3.5
Dynamic Simulation of the Plug-Flow Tubular Reactor

The coupling of the component and energy balance equations in the modelling of non-isothermal tubular reactors can often lead to numerical difficulties, especially in solutions of steady-state behaviour. In these cases, a dynamic digital simulation approach can often be advantageous as a method of determining the steady-state variations in concentration and temperature, with respect to reactor length. The full form of the dynamic model equations are used in this approach, and these are solved up to the final steady-state condition, at which condition

$$\frac{dT}{dt} = \frac{dC_A}{dt} = 0$$

The procedure is to transform the defining model partial differential equation system into sets of difference-differential equations, by dividing the length or volume of the reactor into disc-shaped segments. The concentrations and temperatures at the boundaries of each segment are approximated by a midpoint average. Each segment can therefore be thought of as behaving in a similar manner to that of a well-stirred tank.

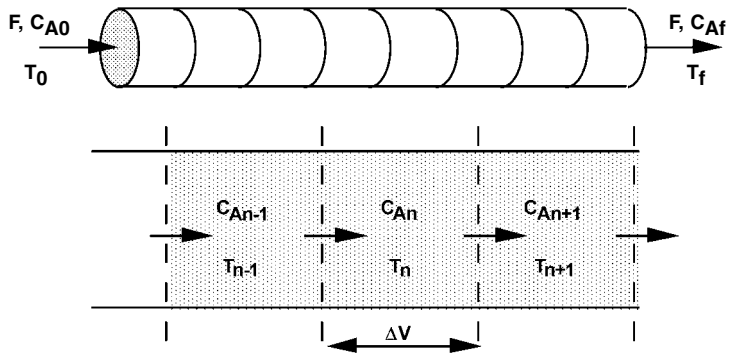

Fig. 4.11 Finite-differencing for a dynamic tubular reactor model.

This is shown above in Fig. 4.11, where segment n, with volume ΔV, is identified by its midpoint concentration C_{An} and midpoint temperature T_n.

The concentration of reactant entering segment n, from segment $n-1$, is approximated by the average of the concentrations in the two segments and is given by

$$\frac{C_{An-1} + C_{An}}{2}$$

Similarly, the concentration of reactant leaving segment n, and entering segment $n+1$, is approximated by

$$\frac{C_{An} + C_{An+1}}{2}$$

This averaging procedure has the effect of improving the approximation. Alternatively, each segment may be treated as a well-mixed tank with the outflow variables equal to the tank values. This simpler approach would require a greater number of segments for the same accuracy.

Applying the generalised component balance equation for component A to each segment n gives

$$\begin{pmatrix}\text{Rate of}\\ \text{Accumulation}\\ \text{of reactant}\end{pmatrix} = \begin{pmatrix}\text{Flow of}\\ \text{reactant}\\ \text{in}\end{pmatrix} - \begin{pmatrix}\text{Flow of}\\ \text{reactant}\\ \text{out}\end{pmatrix} + \begin{pmatrix}\text{Rate of}\\ \text{Production}\\ \text{of reactant}\end{pmatrix}$$

and results in

$$\Delta V \frac{dC_{An}}{dt} = F\left(\frac{C_{An-1} + C_{An}}{2} - \frac{C_{An} + C_{An+1}}{2}\right) + r_{An}\Delta V$$

where $\Delta V = A\,\Delta Z$.

The application of the energy balance equation to segment n results similarly in the relationship

$$\Delta V \rho c_p \frac{dT_n}{dt} = F\rho c_p \left(\frac{T_{n-1} + T_n}{2} - \frac{T_n + T_{n+1}}{2} \right) + \frac{r_{An}}{\nu_A} (-\Delta H) \Delta V - U \Delta A_t (T_n - T_j)$$

where the outer surface area for heat transfer in segment n is given by

$$\Delta A_t = \frac{A_t}{N}$$

A_t is the total surface for heat transfer and for a single tube is given by

$$A_t = \pi D \Delta Z$$

where D is the tube diameter and ΔZ is the length of segment.

The resulting forms of the component and energy balance equations are thus

$$\frac{dC_{An}}{dt} = \frac{C_{An-1} - C_{An+1}}{2\tau_n} + r_{An}$$

$$\frac{dT_n}{dt} = \frac{T_{n-1} - T_{n+1}}{2\tau_n} + \frac{r_{An}}{\nu_A} \frac{(-\Delta H)}{\rho c_p} - \frac{U \Delta A_t (T_n - T_j)}{\Delta V \rho c_p}$$

The above equations are linked by the reaction rate term r_A, which depends on concentration and temperature.

In the above equation, τ_n is the mean residence time in segment n and is equal to the volume of the segment divided by the volumetric flow rate

$$\tau_n = \frac{\Delta V}{F}$$

The modelling of the end sections, however, needs to be handled separately, according to the appropriate boundary conditions. The concentration and temperature conditions at the inlet to the first segment, n=1, are, of course with no axial dispersion, identical to those of the feed, C_{A0} and T_0, which gives rise to a slightly different form of the balance equations for segment 1. The outlet stream conditions may be taken as C_{AN} and T_N or, more accurately, as suggested by Franks (1967), one may assume an extrapolated value of C_{AN+1} and T_{N+1} through segments N−1, N and N+1. This is treated in greater detail in the following section.

4.3.6
Dynamics of an Isothermal Tubular Reactor with Axial Dispersion

Axial and radial dispersion or non-ideal flow in tubular reactors is usually characterised by analogy to molecular diffusion, in which the molecular diffusivity is replaced by eddy dispersion coefficients, characterising both radial and longitudinal dispersion effects. In this text, however, the discussion will be limited to that of tubular reactors with axial dispersion only. Otherwise the model equations become too complicated and beyond the capability of a simple digital simulation language.

Longitudinal diffusion can be analysed using the unsteady-state diffusion equation

$$\frac{\partial C}{\partial t} = -\frac{\partial}{\partial Z}\left(D\frac{\partial C}{\partial Z}\right)$$

based on Fick's Law.

In the above case, D is an eddy dispersion coefficient and Z is the axial distance along the reactor length. When combined with an axial convective flow contribution and considering D as constant the equation takes the form

$$\frac{\partial C}{\partial t} = v\,C - D\frac{\partial^2 C}{\partial Z^2}$$

where v is the linear flow velocity.

Written in dimensionless form, this equation is seen to depend on a dimensionless group vL/D, which is known as the Peclet number. The inverse of the Peclet number is called the Dispersion Number. Both terms represent a measure of the degree of dispersion or axial mixing in the reactor. Thus low values of the Peclet number correspond to high dispersion coefficients, low velocities and short lengths of tube and thus characterise conditions approximating to those of perfect mixing. For high values of the Peclet number the converse conditions apply and thus characterise conditions approximating to perfect plug flow.

In the extreme, the Peclet number corresponds to the following conditions:

$Pe \to 0$ perfect mixing prevails
$Pe \to \infty$ plug flow prevails

4.3.6.1 Dynamic Difference Equation for the Component Balance Dispersion Model

The development of the equations for the dynamic dispersion model starts by considering an element of tube length ΔZ, with a cross-sectional area of A_c, a superficial flow velocity of v and an axial dispersion coefficient or diffusivity D. Convective and diffusive flows of component A enter and leave the element, as shown by the solid and dashed arrows, respectively, in Fig. 4.12.

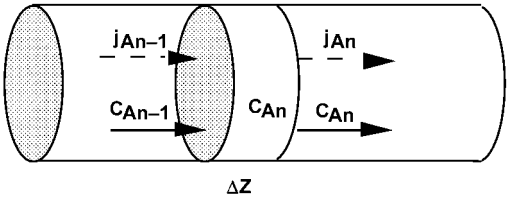

Fig. 4.12 Fluxes for the axial dispersion model.

For each element, the material balance is

$$\begin{pmatrix}\text{Rate of}\\ \text{accumulation}\\ \text{of A}\end{pmatrix} = \begin{pmatrix}\text{Convective}\\ \text{flow of}\\ \text{A in}\end{pmatrix} - \begin{pmatrix}\text{Convective}\\ \text{flow of}\\ \text{A out}\end{pmatrix} + \begin{pmatrix}\text{Diffusive}\\ \text{flow of}\\ \text{A in}\end{pmatrix} - \begin{pmatrix}\text{Diffusive}\\ \text{flow of}\\ \text{A out}\end{pmatrix} - \begin{pmatrix}\text{Rate of}\\ \text{loss of A}\\ \text{due to}\\ \text{reaction}\end{pmatrix}$$

As before, the concentrations are taken as the average in each segment and the diffusion fluxes are related to the concentration gradients at the segment boundaries.

The concentrations of reactant entering and leaving section n are

$$C_{Ain} = \frac{C_{An-1} + C_{An}}{2}$$

and

$$C_{Aout} = \frac{C_{An} + C_{An+1}}{2}$$

The concentration gradients at the inlet and outlet of the section are

$$\left(\frac{dC}{dZ}\right)_{in} = \frac{C_{An-1} - C_{An}}{\Delta Z}$$

and

$$\left(\frac{dC}{dZ}\right)_{out} = \frac{C_{An} - C_{An+1}}{\Delta Z}$$

The convective mass flows in and out are obtained by multiplying the respective concentrations by the volumetric flow rate, which is equal to $A_c v$. The diffusive

mass flows are calculated from the inlet and outlet concentration gradients using the multiplying factor of $A_c D$.

Dropping the A subscript for concentration, the component balance for reactant A, in section n, becomes

$$A_c \Delta Z \frac{dC_n}{dt} = A_c v\left(\frac{C_{n-1} + C_n}{2} - \frac{C_n + C_{n+1}}{2}\right) + \\ + A_c D\left(\frac{C_{n-1} - C_n}{\Delta Z} - \frac{C_n - C_{n+1}}{\Delta Z}\right) - k_n C_n A_c \Delta Z$$

where here the reaction rate is taken as first order, $r_A = k C_A$.

Dividing by $A_c \Delta Z$ gives the defining component material balance equation for segment n, as

$$\frac{dC_n}{dt} = \frac{v}{\Delta Z}\left(\frac{C_{n-1} - C_{n+1}}{2}\right) + D\frac{(C_{n-1} - 2C_n + C_{n+1})}{\Delta Z^2} - k_n C_n$$

A dimensionless form of the balance equation can be obtained by substituting the following dimensionless variables

$$\overline{C}_n = \frac{C_n}{C_0}\,,\ \Delta\overline{Z} = \frac{\Delta Z}{L}\,,\ \bar{t} = \frac{tv}{L}$$

The model for section n, now in dimensionless form, yields

$$\frac{d\overline{C}_n}{d\bar{t}} = \frac{\overline{C}_{n-1} - \overline{C}_{n+1}}{2\Delta\overline{Z}} + \frac{D}{vL}\left(\frac{\overline{C}_{n-1} - 2\overline{C}_n + \overline{C}_{n+1}}{\Delta\overline{Z}^2}\right) - \frac{k_n L}{v\overline{C}_n}$$

where $D/Lv = 1/Pe$, is the inverse Peclet number.

The boundary conditions determine the form of balance equation for the inlet and outlet sections. These require special consideration as to whether diffusion fluxes can cross the boundaries in any particular physical situation. The physical situation of closed ends is considered here. This would be the case if a smaller pipe were used to transport the fluid in and out of the reactor, as shown in Figs. 4.13 and 4.14.

Since no diffusive flux enters the closed entrance of the tube, the component balance for the first section becomes

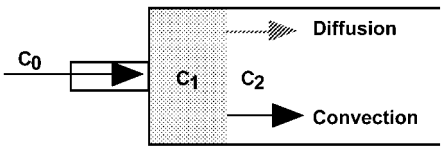

Fig. 4.13 Inlet section for the tubular reactor.

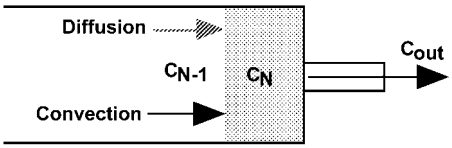

Fig. 4.14 Outlet section of the tubular reactor.

$$A_c\Delta Z\frac{dC_1}{dt} = A_c v\left(C_0 - \frac{C_1 + C_2}{2}\right) - A_c D\frac{(C_1 - C_2)}{\Delta Z} - k_1 C_1 A_c \Delta Z$$

Dividing by $A_c\Delta Z$ gives

$$\frac{dC_1}{dt} = \frac{v(2C_0 - C_1 - C_2)}{2\Delta Z} - D\frac{C_1 - C_2}{\Delta Z^2} - k_1 C_1$$

Similarly, the outlet of the reactor is closed for diffusion as shown in Fig. 4.14.

An extrapolation of the concentration profile over the last half of element N is used to calculate the outlet concentration C_{out}, giving

$$C_{out} = C_N - \frac{C_{N-1} - C_N}{2}$$

with the balance for section N becoming

$$A_c\Delta Z\frac{dC_N}{dt} = A_c v(C_{N-1} - C_N) + \frac{A_c D}{\Delta Z}(C_{N-1} - C_N) - k_N C_N A_c \Delta Z$$

$$\frac{dC_N}{dt} = v\frac{C_{N-1} - C_N}{\Delta Z} + D\frac{C_{N-1} - C_N}{\Delta Z^2} - k_N C_N$$

A similar finite-differenced equivalent for the energy balance equation (including axial dispersion effects) may be derived. The simulation example DISRET involves the axial dispersion of both mass and energy and is based on the work of Ramirez (1976). A related model without reaction is used in the simulation example FILTWASH.

4.3.7
Steady-State Tubular Reactor Dispersion Model

Letting the element distance ΔZ approach zero in the finite-difference form of the dispersion model, gives

$$\frac{\partial C_A}{\partial t} = -v\frac{\partial C_A}{\partial Z} + D\frac{\partial^2 C_A}{\partial Z^2} - kC_A$$

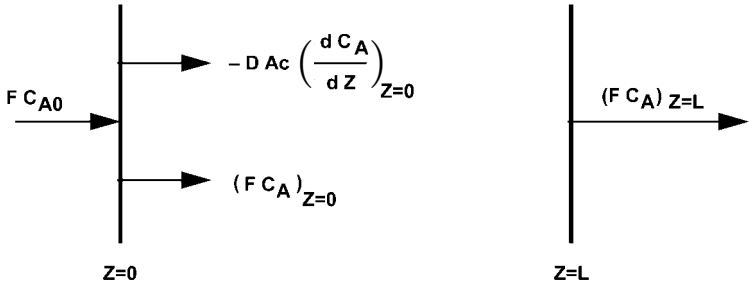

Fig. 4.15 Convective and diffusive fluxes at the entrance (Z=0) and exit (Z=L) of the tubular reactor.

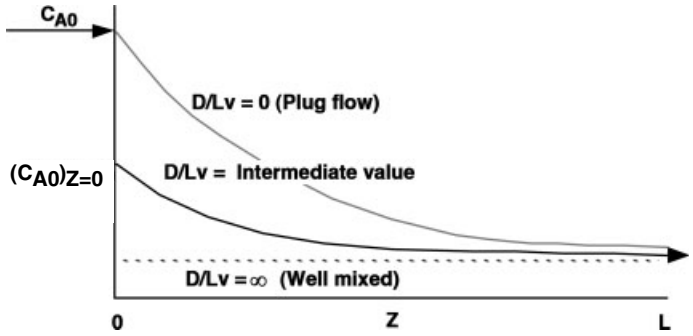

Fig. 4.16 Concentration profiles in the tubular reactor for extreme and intermediate values of the dispersion number.

Defining the following dimensionless variables

$$\overline{C}_A = \frac{C_A}{C_{A0}}\,,\ \overline{Z} = \frac{Z}{L}\,,\ \bar{t} = \frac{t}{\tau}$$

where $\tau = L/v$.

The dimensionless form for an nth-order reaction is

$$\frac{\partial \overline{C}_A}{\partial \bar{t}} = -\frac{\partial \overline{C}_A}{\partial \overline{Z}} - \left(\frac{D}{Lv}\right)\frac{\partial^2 \overline{C}_A}{\partial \overline{Z}^2} - k\tau C_{A0}^{n-1}(\overline{C}_A)^n$$

At steady state $\partial \overline{C}_A/\partial \bar{t}$ can be set to zero and the equation becomes an ordinary second-order differential equation, which can be solved using MADONNA.

Again the entrance and exit boundary conditions must be considered. Thus the two boundary conditions at Z=0 and Z=L are used for solution, as shown in Fig. 4.15. Note that these boundary conditions refer to the inner side of the tubular reactor. A discontinuity in concentration at Z=0 is apparent in Fig. 4.16.

Balancing the material flows at the inlet gives a relation for the boundary conditions at $Z=0$

$$FC_{A0} = (FC_A)_{Z=0} - DA_c\left(\frac{dC_A}{dZ}\right)_{Z=0}$$

The zero flux condition at the closed outlet requires a zero gradient, thus

$$\left(\frac{dC_A}{dZ}\right)_{Z=L} = 0$$

According to the boundary conditions, the concentration profile for A must change with a discontinuity in concentration from C_{A0} to $(C_{A0})_{Z=0}$ occurring at the reactor entrance, as shown in Fig. 4.16.

In dimensionless form the boundary condition at $\overline{Z}=0$ is represented by

$$\overline{C}_A - \frac{D}{Lv}\frac{d\overline{C}_A}{d\overline{Z}} = 1$$

and at $\overline{Z}=1$ by $\dfrac{d\overline{C}_A}{d\overline{Z}} = 0$.

The solution requires two integrations as shown in Fig. 4.17.

Referring to Fig. 4.15, it is seen that the concentration and the concentration gradient are unknown at $Z=0$. The above boundary condition relation indicates that if one is known, the other can be calculated. The condition of zero gradient at the outlet ($Z=L$) does not help to start the integration at $Z=0$, because, as Fig. 4.17 shows, two initial conditions are necessary. The procedure to solve this split-boundary value problem is therefore as follows:

1. Guess $(\overline{C}_A)_{Z=0}$ and calculate $\left(\dfrac{d\overline{C}_A}{d\overline{Z}}\right)_{\overline{Z}=0}$ from the boundary condition relation.
2. Integrate to $\overline{Z}=1$ and check whether $\left(\dfrac{d\overline{C}_A}{d\overline{Z}}\right)_{\overline{Z}=1}$ equals zero.
3. Vary the guess and iterate between $\overline{Z}=0$ and $\overline{Z}=1$ until convergence is obtained.

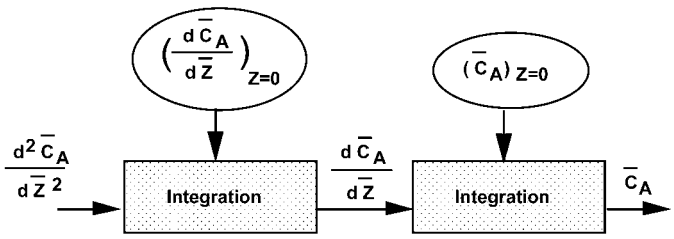

Fig. 4.17 Flow diagram for solving the second-order differential equation from the axial dispersion model.

4.4
Differential Mass Transfer

This section concerns the modelling of countercurrent flow, differential mass transfer applications, for both steady-state and non-steady-state design or simulation purposes. For simplicity, the treatment is restricted to the case of a single solute, transferring between two inert phases, as in the standard treatments of liquid–liquid extraction or gas absorption column design.

4.4.1
Steady-State Gas Absorption with Heat Effects

Figure 4.18 represents a countercurrent-flow, packed gas absorption column, in which the absorption of solute is accompanied by the evolution of heat. In order to treat the case of concentrated gas and liquid streams for which total flow rates of both gas and liquid vary throughout the column, the solute concentrations in the gas and liquid are defined in terms of mole ratio units and related to the molar flow rates of solute free gas and liquid respectively, as discussed previously in Section 3.3.2. By convention, the mass transfer rate equation is however expressed in terms of mole fraction units. In Fig. 4.18, G_m is the molar flow of solute free gas (kmol/m^{2}s) and L_m is the molar flow of solute free liquid (kmol/m^{2}s), where both L_m and G_m remain constant throughout the column. Y is the mole ratio of solute in the gas phase (kmol solute/kmol solute free gas), X is the mole ratio of solute in the liquid phase (kmol solute/kmol solute free liquid), y is the mole fraction of solute in the gas phase, x is the mole fraction of solute in the liquid phase and T is temperature (K).

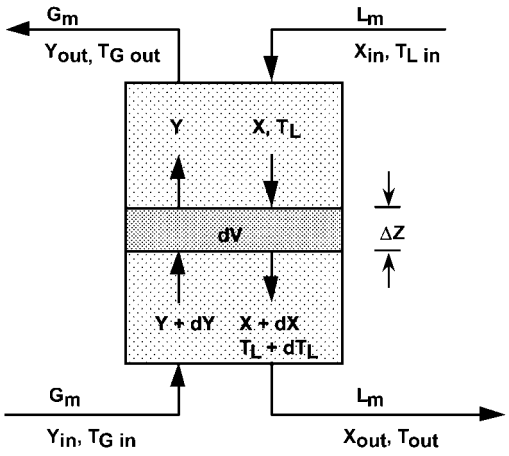

Fig. 4.18 Steady-state gas absorption with heat effects.

Mole ratio and mole fraction contents are related by

$$Y = \frac{y}{1-y} \quad \text{and} \quad X = \frac{x}{1-x}$$

$$x = \frac{Y}{1+Y} \quad \text{and} \quad y = \frac{X}{1+X}$$

Subscripts L and G refer to the liquid and gas phases, respectively, and subscripts 'in' and 'out' refer to the inlet and outlet streams.

4.4.1.1 Steady-State Design

In the steady-state design application, the flow rates L_m and G_m and concentrations Y_{in}, X_{in}, Y_{out} and X_{out} will either be specified or established by an overall steady-state solute balance, where

$$L_m X_{in} + G_m Y_{in} = L_m X_{out} + G_m Y_{out}$$

Temperatures T_{Lin} and T_{Gin} will also be known. The problem then consists of determining the height of packing required to obtain the above separation.

Component Material Balance Equations

For a small element of column volume dV

$$\begin{pmatrix} \text{Rate of loss} \\ \text{of solute from} \\ \text{the gas} \end{pmatrix} = \begin{pmatrix} \text{Rate of gain} \\ \text{of solute in} \\ \text{the liquid} \end{pmatrix} = \begin{pmatrix} \text{Rate} \\ \text{of solute} \\ \text{transfer} \end{pmatrix}$$

$$-G_m A_c dY = L_m A_c dX = K_{Lx} a(x^* - x) dV$$

Here $K_{Lx}a$ (kmol/m^{3}s) is the overall mass transfer coefficient for the liquid phase, based on mole fraction in the L-phase, x^* is the equilibrium liquid phase mole fraction, and A_c is the cross-sectional area of the column (m^2). Hence with $dV = A_c\, dZ$

$$\frac{dY}{dZ} = \frac{K_{Lx} a(x^* - x)}{G_m}$$

and

$$\frac{dX}{dZ} = \frac{K_{Lx} a(x^* - x)}{L_m}$$

Energy Balance

It is assumed that there are no heat losses from the column and that there is zero heat exchange between the gas and liquid phases. Consequently the gas phase temperature will remain constant throughout the column. A liquid phase heat balance for element of volume dV is given by

$$\begin{pmatrix}\text{Rate of gain of heat}\\ \text{by the liquid}\end{pmatrix} = \begin{pmatrix}\text{Rate of generation of}\\ \text{heat by absorption}\end{pmatrix}$$

or

$$L\,A_c\,c_p\,dT_L = K_{Lx}\,a\,(x^* - x)\,dV\Delta H_{abs}$$

where L is the total mass flow rate of liquid (kg/m^2 s), c_p is the specific heat capacity of the liquid (kJ/kg K) and ΔH_{abs} is the exothermic heat of absorption (kJ/kmol solute transferred). Hence

$$\frac{dT_L}{dZ} = \frac{K_{Lx}\,a(x^* - x)\Delta H_{abs}}{Lc_p}$$

The temperature variation throughout the column is important, since this affects the equilibrium concentration x^*, where

$$x^* = f_{eq}(y, T_L)$$

Solution of the required column height is achieved by integrating the two component balance equations and the heat balance equation down the column from the known conditions x_{in}, y_{out} and T_{Lin}, until the condition that either Y is greater than Y_{in} or X is greater than X_{out} is achieved. In this solution approach, variations in the overall mass transfer capacity coefficient both with respect to temperature and to concentration, if known, can also be included in the model as required. The solution procedure is illustrated by the simulation examples AMMONAB and BIOFILT.

Using the digital simulation approach to steady-state design, the above design calculation is shown to proceed naturally from the defining component balance and energy balance equations, giving a considerable simplification to conventional text book approaches.

4.4.1.2 Steady-State Simulation

In this case, the flow rates L_m and G_m, concentrations Y_{in} and X_{in}, temperatures T_{Gin} and T_{Lin}, are known and in addition the height of packing Z is also known. It is now, however, required to establish the effective column performance by determining the resulting steady-state concentration values, Y_{out} and X_{out}, and also temperature T_{Lout}. The problem is now of a split-boundary type

and must be solved by assuming a value for Y_{out}, integrating down the column for a column distance Z and comparing the calculated value for Y_{in} with the known inlet gas concentration condition. A revised guess for the starting value Y_{out} can then be taken and the procedure repeated until convergence is achieved. This is easy using MADONNA's split boundary tool.

4.4.2 Dynamic Modelling of Plug-Flow Contactors: Liquid–Liquid Extraction Column Dynamics

A plug-flow, liquid–liquid, extraction column is represented in Fig. 4.19. For convenience, it is assumed that the column operates under low concentration conditions, such that the aqueous and organic flow rates, L and G, respectively are constant. At low concentration, mole fraction x and y are identical to mole ratios X and Y, which are retained here in the notation for convenience. This however leads to a more complex formulation than when concentration quantities are used, as in the example AXDISP.

Consider a differential element of column volume ΔV, height ΔZ and cross-sectional area, A_c, such that $\Delta V = A_c \Delta Z$. Component material balance equations can be written for each of the liquid phases, where

$$\begin{pmatrix}\text{Rate of}\\ \text{accumulation}\\ \text{of solute}\end{pmatrix} = \begin{pmatrix}\text{Convective}\\ \text{flow of}\\ \text{solute in}\end{pmatrix} - \begin{pmatrix}\text{Convective}\\ \text{flow of}\\ \text{solute out}\end{pmatrix} + \begin{pmatrix}\text{Rate of}\\ \text{solute}\\ \text{transfer}\end{pmatrix}$$

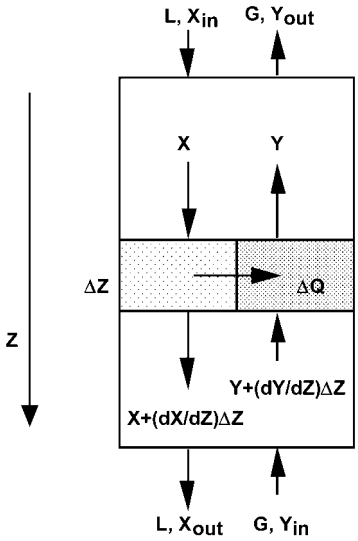

Fig. 4.19 Liquid–liquid extraction column dynamic representation.

The actual volume of each phase in element ΔV is that of the total volume of the element, multiplied by the respective fractional phase holdup. Hence considering the direction of solute transfer to occur from the aqueous or feed phase into the organic or solvent phase, the material balance equations become:

For the aqueous phase

$$\rho_L h_L \Delta V \frac{\partial X}{\partial t} = -LA_c \frac{\partial X}{\partial t} \Delta Z - K_{LX}\, a\, (X - X^*) \Delta V$$

for the organic phase

$$\rho_G h_G \Delta V \frac{\partial Y}{\partial t} = GA_c \frac{\partial Y}{\partial Z} \Delta Z + K_{LX}\, a\, (X - X^*) \Delta V$$

where each term in the equations has units of kmol solute/s and where the symbols are as follows:

- a is the specific interfacial area related to the total volume (m^2/m^3)
- A_c is the column cross-sectional area (m^2)
- G is the molar flow rate of the light, organic phase per unit area ($kmol/m^2 s$)
- h_G is the volumetric holdup fraction of the light organic phase (–)
- h_L is the volumetric holdup fraction of the heavy aqueous phase (–)
- $K_{LX}a$ is the overall mass transfer capacity coefficient based on the aqueous phase mole ratio X ($kmol/m^3 s$)
- L is the molar flow rate of the heavy aqueous phase per unit area ($kmol/m^2 s$)
- X is the aqueous phase mole ratio (kmol solute/kmol water)
- X^* is the equilibrium mole ratio in the heavy phase, corresponding to light phase mole ratio Y (kmol solute/kmol water)
- Y is the organic phase mole ratio (kmol solute/kmol organic)
- Z is the height of the packing (m)
- ΔV is the total volume of one column segment with length ΔZ (m^3)
- ρ_G is the density of the solute-free light phase ($kmol/m^3$)
- ρ_L is the density of the solute-free heavy phase ($kmol/m^3$)

The above balance equations simplify to

$$\rho_L h_L \frac{\partial X}{\partial t} = L \frac{\partial X}{\partial Z} - K_{LX}\, a (X - X^*)$$

$$\rho_G h_G \frac{\partial Y}{\partial t} = -G \frac{\partial Y}{\partial Z} + K_{LX}\, a (X - X^*)$$

with the equilibrium relationship represented by

$$X^* = f_{eq}(Y)$$

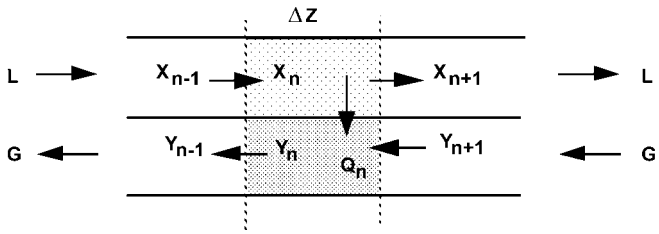

Fig. 4.20 Finite-difference element for the two-phase transfer system.

Thus the system is defined by two coupled partial differential equations, which can be solved by finite-differencing.

Consider a finite-difference element of length ΔZ as shown in Fig. 4.20.

Approximating the concentrations entering and leaving each section by an arithmetical mean of the neighbouring concentrations, as shown in Section 4.3.5, the component balance equations for stage n become

$$\rho_L h_L A_c \Delta Z \frac{dX_n}{dt} = LA_c\left(\frac{(X_{n-1}+X_n)}{2} - \frac{(X_n+X_{n+1})}{2}\right) - Q_n$$

and

$$\rho_G h_G A_c \Delta Z \frac{dY_n}{dt} = GA_c\left(\frac{(Y_{n+1}+Y_n)}{2} - \frac{(Y_n+Y_{n-1})}{2}\right) + Q_n$$

where Q_n (kmol solute/s) is rate of solute transfer in element n given by

$$Q_n = K_{LX}\, a\, (X - X^*)\Delta V$$

Hence with $\Delta V = A_c \Delta Z$

$$\rho_L h_L \frac{dX_n}{dt} = -L\frac{(X_{n+1}-X_{n-1})}{2\Delta Z} - K_{LX}\, a\, (X - X^*)$$

$$\rho_G h_G \frac{dY_n}{dt} = -G\frac{(Y_{n+1}-Y_{n-1})}{2\Delta Z} + K_{LX}\, a\, (X - X^*)$$

The boundary conditions are formulated with the help of Figs. 4.21 and 4.22 and in accordance with the methodology of Franks (1967).

This gives for stage 1

$$\rho_L h_L \frac{dX_1}{dt} = \frac{L}{2\Delta Z}(2X_0 - X_1 - X_2) - K_{LX}\, a\, (X_1 - X_1^*)$$

$$\rho_G h_G \frac{dY_1}{dt} = \frac{G}{2\Delta Z}(Y_2 + Y_1 - 2Y_0) + K_{LX}\, a\, (X_1 - X_1^*)$$

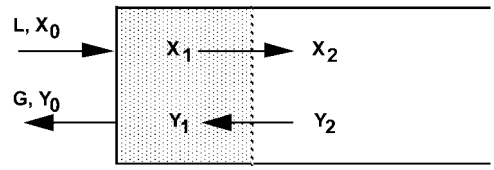

Fig. 4.21 Aqueous and organic phase streams at the inlet.

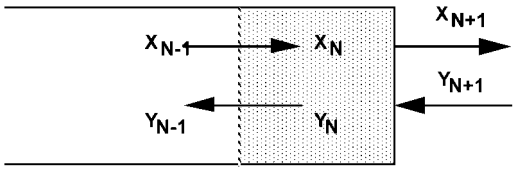

Fig. 4.22 Aqueous and organic phase streams at the outlet.

The balances for the end stage N thus become

$$\rho_L h_L \frac{dX_N}{dt} = \frac{L}{2\Delta Z}(X_{N-1} - X_N - 2X_{N+1}) - K_{LX}\, a\, (X_N - X_N^*)$$

$$\rho_G h_G \frac{dY_N}{dt} = \frac{G}{2\Delta Z}(Y_{N+1} - Y_N - Y_{N-1}) + K_{LX}\, a\, (X_N - X_N^*)$$

The representation of the boundary conditions for both the top and bottom of the column are really more mathematical than practical in nature and fail to take into account the actual geometry and construction of the upper and lower parts of the column and the relative positioning of the inlet and outlet connections. They may therefore require special modelling appropriate to the particular form of construction of the column, as discussed previously in Section 3.3.1.10.

4.4.3
Dynamic Modelling of a Liquid–Liquid Extractor with Axial Mixing in Both Phases

Axial mixing is known to have a very significant effect on the performance of agitated liquid–liquid extraction columns, and any realistic description of column performance must take this into account. Figure 4.23 represents a small differential element of column volume ΔV and height ΔZ. Here the convective flow rates, as in Fig. 4.19, are shown by the solid arrows, and the additional dispersion contributions, representing axial mixing, are shown by dashed arrows. It is assumed that axial mixing in both phases can be described by analogy to Fick's Law, but using an effective eddy dispersion coefficient appropriate to the respective liquid phase.

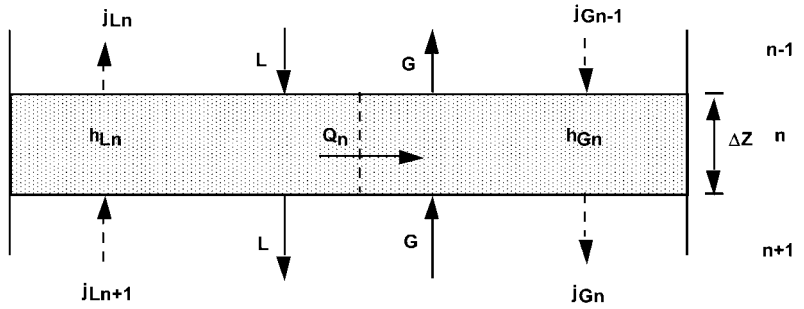

Fig. 4.23 Differential element of height, ΔZ, for a liquid–liquid extractor with axial mixing in both phases.

Writing unsteady-state component balances for each liquid phase results in the following pair of partial differential equations which are linked by the mass transfer rate and equilibrium relationships

$$\rho_L h_L \frac{\partial X}{\partial t} = -L\frac{\partial X}{\partial Z} + \rho_L h_L D_L \frac{\partial^2 X}{\partial Z^2} - K_{LX}\, a\, (X - X^*)$$

$$\rho_G h_G \frac{\partial Y}{\partial t} = G\frac{\partial Y}{\partial Z} + \rho_G h_G D_G \frac{\partial^2 Y}{\partial Z^2} + K_{LX}\, a\, (X - X^*)$$

Here the nomenclature is the same as in Section 4.4.2. In addition, D_G is the effective eddy dispersion coefficient for the organic or extract phase (m^2/s) and D_L is the effective eddy dispersion coefficient for the aqueous or feed phase (m^2/s). The above equations are difficult to solve analytically (Lo et al., 1983) but are solved with ease using digital simulation.

Referring to Fig. 4.23, the extractor is again divided into N finite-difference elements or segments of length ΔZ. The convective terms are formulated for each segment using average concentrations entering and leaving the segment, as shown in Section 4.4.2. The backmixing terms j are written in terms of dispersion coefficients times driving-force mole-ratio gradients. The resulting equations for any segment n are then for the aqueous feed phase with each term in kmol solute/s.

$$\rho_L h_{Ln} \Delta Z A_c \frac{dX_n}{dt} = LA_c\left(\frac{X_n + X_{n-1}}{2} - \frac{X_{n+1} + X_n}{2}\right) +$$

$$+ \rho_L D_L h_{Ln} A_c\left(\frac{X_{n+1} - X_n}{\Delta Z} - \frac{X_n - X_{n-1}}{\Delta Z}\right) - K_{LXn}\, a_n\, (X_n - X_n^*)\Delta Z A_c$$

Rearranging

$$\frac{dX_n}{dt} = -\frac{L}{2h_{Ln}\rho_L \Delta Z}(X_{n+1} - X_{n-1}) + \frac{D_L}{\Delta Z^2}(X_{n+1} - 2X_n + X_{n-1}) - \\ - \frac{K_{LXn}\, a_n}{h_{Ln}\rho_L}(X_n - X_n^*)$$

Similarly for the light solvent–extract phase

$$\Delta Z A_c h_{Gn}\rho_G \frac{dY_n}{dt} = A_c G\left(\frac{Y_n + Y_{n+1}}{2} - \frac{Y_{n-1} + Y_n}{2}\right) + \\ + \rho_G D_G h_{Gn} A_c\left(\frac{Y_{n-1} - Y_n}{\Delta Z} - \frac{Y_n - Y_{n+1}}{\Delta Z}\right) + K_{LXn}\, a_n\,(X_n - X_n^*)\Delta Z A_c$$

Rearranging

$$\frac{dY_n}{dt} = \frac{G}{2h_{Gn}\rho_G \Delta Z}(Y_{n+1} - Y_{n-1}) + \frac{D_G}{\Delta Z^2}(Y_{n+1} - 2Y_n + Y_{n-1}) - \frac{K_{LXn}\, a_n}{h_{Gn}\rho_G}(X_n - X_n^*)$$

Note that the above formulation includes allowance for the fractional phase holdup volumes, h_L and h_G, the phase flow rates, L and G, the diffusion coefficients D_L and D_G, and the overall mass transfer capacity coefficient K_{LX} a, all of which may vary with position along the extractor.

Boundary Conditions

The column end sections require special treatment to allow for the fact that zero diffusive flux enters through the end wall of the column. The equations for the end section are derived by setting the diffusion flux leaving the column to zero. In addition, the liquid phase outlet concentrations leaving the respective end sections of the column are approximated by an extrapolation of the concentration gradient from the preceding section. The resulting model equations give the concentrations of each segment in both phases as well as the outlet concentrations as a function of time. The resulting model formulation is shown in the simulation example AXDISP.

4.4.4
Dynamic Modelling of Chromatographic Processes

Preparative chromatographic processes are of increasing importance particularly in the production of fine chemicals. A mixture of compounds is introduced into the liquid mobile phase, and this then flows through a packed column containing the stationary solid phase. The contacting scheme is thus differential, but since the adsorption characteristics of the compounds in the mixture are similar, many equivalent theoretical stages are required for their separation. Chromatographic processes are mostly run under transient conditions, such that

concentration variations occur with respect to both time and space, but steady-state and quasi-steady-state systems are also being applied increasingly to overcome the inherent disadvantages of batch operation. The transient operational mode is essentially a scaled-up version of the usual analytical chromatography, but whereas analytical systems are usually run with low concentrations to avoid non-linearities, preparative industrial systems are highly loaded to increase productivity. Countercurrent chromatography is still not available, but simulated moving bed chromatography with switching between a series of columns is used increasingly industrially. An important feature of chromatographic process behaviour is that it is generally governed more by the adsorption equilibrium than by the kinetics of adsorption.

The modelling of chromatographic processes is treated in great detail by Ruthven and Ching (1993) and by Blanch and Clark (1996), with two alternative approaches being available. In a most rigorous approach the chromatographic separation column is considered as a plug flow contactor with axial dispersion analogous to previous descriptions in this chapter (Section 4.3.6). The second approach is to represent the column as a large number of well mixed stages, with a treatment similar to that shown in Chapter 3.

The interaction of the two phases can be accomplished either through the assumption of equilibrium or through a transfer rate that will eventually reach equilibrium. The transfer rate approach is closer to the real process and simplifies the calculations for nonlinear equilibrium. This is similar to the modelling of extraction columns with backmixing as found in Section 4.4.3. For linear equilibrium, simplifications in the models are possible. In the following section, the dispersion model is developed and is presented as a simulation example CHROMDIFF. A further simulation example, CHROMPLATE, considers the stagewise model for linear equilibrium. Dynamic modelling and simulation of simulated moving bed chromatography has been studied by Storti et al. (1993) and Strube et al. (1998).

4.4.4.1 Axial Dispersion Model for a Chromatography Column

Generally for modelling chromatograph systems, component mass balances are required for each component in each phase. The differential liquid phase component balances for a chromatographic column with non-porous packing take the partial differential equation form

$$\frac{\partial C_L}{\partial t} = -v\frac{\partial C_L}{\partial Z} + D\frac{\partial^2 C_L}{\partial Z^2} - \frac{1-\varepsilon}{\varepsilon} r_{ads}$$

where C_L is the liquid phase concentration of each component and D is the axial dispersion coefficient.

The linear superficial flow velocity in the packing voids v is calculated from volumetric flow rate L_{in}, voidage fraction of the adsorbant bed ε and column diameter d as

$$v = \frac{4L_{in}}{\varepsilon \pi d^2}$$

The transfer rate of the sorbate from the liquid phase to the solid adsorbant r_{ads} can be written as

$$r_{ads} = k(C_S^* - C_S)$$

Here the rate is specific to a unit volume of solids ($g/cm^3 s$) and k is a mass transfer rate coefficient (1/s).

The solid phase concentrations are influenced only by the rate of mass transfer, with convection and dispersion effects both being zero for this phase.

$$\frac{\partial C_S}{\partial t} = \frac{1-\varepsilon}{\varepsilon} r_{ads}$$

Equilibrium relations are required to calculate the values of C_S^*, the solid phase equilibrium concentrations, for each component. For very dilute systems these relations may be of linear form

$$C_S^* = KC_L$$

where K is the equilibrium constant for the particular component.

For concentrated systems the Langmuir adsorption form may be appropriate and for an interacting two-component system (A and B) may take the form

$$C_{SA}^* = \frac{K_A C_{LA}}{1 + b_A C_{LA} + b_B C_{LB}}$$

$$C_{SB}^* = \frac{K_B C_{LB}}{1 + b_A C_{LA} + b_B C_{LB}}$$

Here the constants b_A and b_B account for the competitive adsorption effects between components A and B.

Writing the model in dimensionless form, the degree of axial dispersion of the liquid phase will be found to depend on a dimensionless group vL/D or Peclet number. This is completely analogous to the case of the tubular reactor with axial dispersion (Section 4.3.6).

4.4.4.2 **Dynamic Difference Equation Model for Chromatography**

Instead of the partial differential equation model presented above, the model is developed here in dynamic difference equation form, which is suitable for solution by dynamic simulation packages, such as MADONNA. Analogous to the previous development for tubular reactors and extraction columns, the development of the dynamic dispersion model starts by considering an element of tube

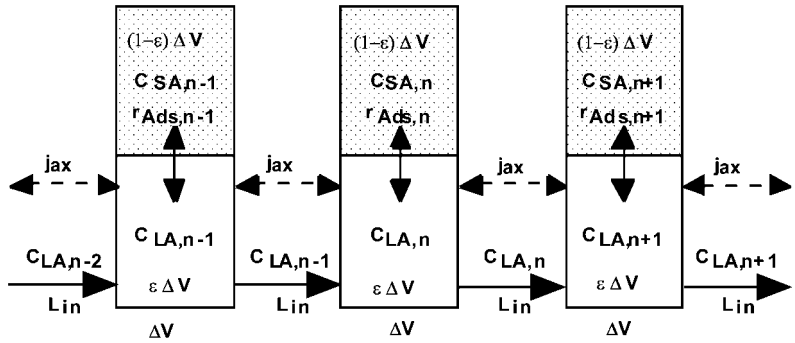

Fig. 4.24 Finite difference axial dispersion model of a chromatographic column.

length ΔZ, with a cross-sectional area A_c, a superficial flow velocity v and an axial dispersion coefficient or diffusivity D. Convective and diffusive flows of component A enter and leave the liquid phase volume of any element n, as indicated in Fig. 4.24 below. Here j represents the diffusive flux, L the liquid flowrate and C_{SA} and C_{LA} the concentration of any species A in both the solid and liquid phases, respectively.

For each element, the material balance in the liquid phase, here for component A, is

$$\begin{pmatrix}\text{Rate of}\\ \text{acumulation}\\ \text{of component}\\ \text{A}\end{pmatrix} = \begin{pmatrix}\text{Convective}\\ \text{flow of}\\ \text{A in}\end{pmatrix} - \begin{pmatrix}\text{Convective}\\ \text{flow of}\\ \text{A out}\end{pmatrix} + \begin{pmatrix}\text{Diffusive}\\ \text{flow of}\\ \text{A in}\end{pmatrix} - \begin{pmatrix}\text{Diffusive}\\ \text{flow of}\\ \text{A out}\end{pmatrix} + \begin{pmatrix}\text{Rate of}\\ \text{loss of A due}\\ \text{to transfer}\end{pmatrix}$$

As before, the concentrations are taken as the average in each segment and the diffusion fluxes are related to the concentration gradients at the segment boundaries.

The concentrations of reactant entering and leaving any section n are

$$C_{LA,\,in} = \frac{C_{LA,\,n-1} + C_{LA,\,n}}{2}$$

and

$$C_{LA,\,out} = \frac{C_{LA,\,n} + C_{LA,\,n+1}}{2}$$

The concentration gradients at the inlet and outlet of the section are

$$\left(\frac{dC_{LA}}{dZ}\right)_{in} = \frac{C_{LA,n-1} - C_{LA,n}}{\Delta Z}$$

and

$$\left(\frac{dC_{LA}}{dZ}\right)_{out} = \frac{C_{LA,n} - C_{LA,n+1}}{\Delta Z}$$

The convective mass flows in and out of the segment are calculated by multiplying the respective concentrations by the constant volumetric flow rate, L_{in}. The diffusive mass flows are calculated from Fick's Law, using the inlet and outlet concentration gradients and the area εA_c.

The transfer rate of A, Tr_A (g/s), from liquid to solid is given by

$$Tr_A = r_{Aads}\Delta V_S = k_{eff}\, a_p\, (C^*_{SA} - C_{SA})(1-\varepsilon)\Delta Z A_c$$

where k_{eff} (cm/s) is a transfer coefficient, a_p is the specific area of the spherical packing ($6/d_p$) and ΔV_S is the volume of the solid phase. C^*_{SA} is given by the equilibrium relation

$$C^*_{SA} = f_{equil}(C_{LA})$$

The component balance for reactant A in the liquid phase, in any section n, becomes

$$\varepsilon A_c \Delta Z \frac{dC_{LA,n}}{dt} = L_{in}\left(\frac{C_{LA,n-1} + C_{LA,n}}{2} - \frac{C_{LA,n} + C_{LA,n+1}}{2}\right) +$$

$$+ \varepsilon A_c D\left(\frac{C_{LA,n-1} - C_{LA,n}}{\Delta Z} - \frac{C_{LA,n} - C_{LA,n+1}}{\Delta Z}\right) - (1-\varepsilon) r_{Aads}\Delta Z A_c$$

Here the specific transfer rate r_{ads} is related to the solid phase volume.

Dividing by $\varepsilon A_c \Delta Z$ gives the defining component material balance equation for segment n as

$$\frac{dC_{LA,n}}{dt} = \frac{L_{in}}{\varepsilon A_c \Delta Z}\left(\frac{C_{LA,n-1} - C_{LA,n+1}}{2}\right) +$$

$$+ D\frac{(C_{LA,n-1} - 2C_{LA,n} + C_{LA,n+1})}{\Delta Z^2} - \frac{1-\varepsilon}{\varepsilon} r_{Aads,n}$$

A dimensionless form of the balance equation can be obtained in the same way as described for the tubular reactor (Section 4.3.6).

The balance equation for component A in the solid phase balance for any element n is

$$(1-\varepsilon)A_c\Delta Z\frac{dC_{SA,n}}{dt} = (1-\varepsilon)A_c\Delta Z\, r_{Aads,n}$$

or simply

$$\frac{dC_{SA,n}}{dt} = r_{Aads,n}$$

The formulation of the end section balances needs special attention as already discussed in Section 4.3.6.1.

The axial dispersion coefficient may be calculated from a knowledge of the Peclet number, where

$$D = \frac{4L_{in}D_p}{Pe\,\varepsilon\,\pi\,d^2}$$

The Reynolds number for a particle with diameter D_p is defined as

$$Re = \frac{\rho\, v\, D_p}{\eta}$$

and this is used to determine the Peclet number from a suitable correlation, such as

$$Pe = \frac{0.2}{\varepsilon} + \frac{0.011}{\varepsilon}\left(\frac{Re}{\varepsilon}\right)^{0.48}$$

These equations are applied in the simulation example CHROMDIFF to the case of a two-component separation with linear equilibrium. The situation of a non-linear equilibrium is considered as an exercise in the example.

The simulation program CHROMPLATE uses the plate model for the same column conditions as the simulation model CHROMDIFF. The results obtained are very similar in the two approaches, but the stagewise model is much faster to calculate.

With high concentrations, heat effects in the chromatographic column may be important. This would require the simultaneous application of an energy balance and the introduction of a term reflecting the influence of temperature on the adsorption equilibrium.

4.5
Heat Transfer Applications

4.5.1
Steady-State Tubular Flow with Heat Loss

Here a steady-state formulation of heat transfer is considered (Pollard, 1978). A hot fluid flows with linear velocity v, through a tube of length L, and diameter D, such that heat is lost via the tube wall to the surrounding atmosphere. It is required to find the steady-state temperature profile along the tube length.

Consider an element of tube of length ΔZ, distance Z from the tube inlet as shown in Fig. 4.25. If the temperature at the inlet to the tube element is T, then the temperature at the outlet of the element can be written as $T + (dT/dZ)\,\Delta Z$.

The energy balance for the element of tube length can be stated as

$$\begin{pmatrix}\text{Rate of}\\ \text{accumulation}\\ \text{of enthalpy}\\ \text{in the element}\end{pmatrix} = \begin{pmatrix}\text{Heating of}\\ \text{inlet stream}\\ \text{to element}\\ \text{temperature}\end{pmatrix} - \begin{pmatrix}\text{Rate of}\\ \text{heat loss}\\ \text{to the wall}\end{pmatrix}$$

As shown in Section 1.2.5 the heat balance equation, assuming constant fluid properties, becomes

$$Mc_p \frac{dT}{dt} = Wc_p\left(T - \left(T + \frac{dT}{dZ}\Delta Z\right)\right) - U\,A\,(T - T_w)$$

where

A is the heat transfer surface area for the element = $2\pi D\,\Delta Z$ (m^2)
D is the tube diameter (m)
M is mass of fluid in the element = $(\pi D^2/4)\rho\Delta Z$ (kg)
T_s is the wall temperature (K)
T_w is the temperature of the wall (K)
U is the heat transfer coefficient between the fluid and the wall ($kJ/m^2 s$)
v is the linear velocity of the fluid (m/s)
W is the mass flow rate along the tube = $(\pi D^2/4)\rho v$ (kg/s)

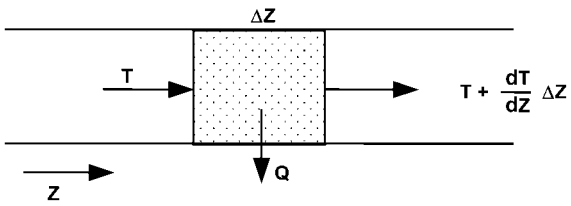

Fig. 4.25 Tubular flow with heat loss.

Simplifying the above equation gives

$$\frac{dT}{dt} = -v\frac{dT}{dZ} - \frac{4U}{\rho c_p D}(T - T_w)$$

Under steady-state conditions, $\frac{dT}{dt} = 0$, and the resulting temperature profile along the tube is given by

$$v\frac{dT}{dZ} + \frac{4U}{\rho c_p D}(T - T_s) = 0$$

Assuming constant coefficients, both the dynamic and steady-state equations describing this system can be solved analytically, but the case of varying coefficients requires solution by digital simulation.

4.5.2
Single-Pass, Shell-and-Tube, Countercurrent-Flow Heat Exchanger

4.5.2.1 Steady-State Applications

Figure 4.26 represents a steady-state, single-pass, shell-and-tube heat exchanger. For this problem W is the mass flow rate (kg/s), T is the temperature (K), c_p is the specific heat capacity (kJ/m^2 s), A ($=\pi D Z$) is the heat transfer surface area (m^2), and U is the overall heat transfer coefficient (kJ/m^2 s K). Subscripts c and h refer to the cold and hot fluids, respectively.

Heat balances on a small differential element of heat transfer surface area, ΔA, give

$$\begin{pmatrix}\text{Rate of}\\ \text{accumulation}\\ \text{of enthalpy}\\ \text{in the element}\end{pmatrix} = \begin{pmatrix}\text{Rate of}\\ \text{heat transfer}\\ \text{to the element}\end{pmatrix}$$

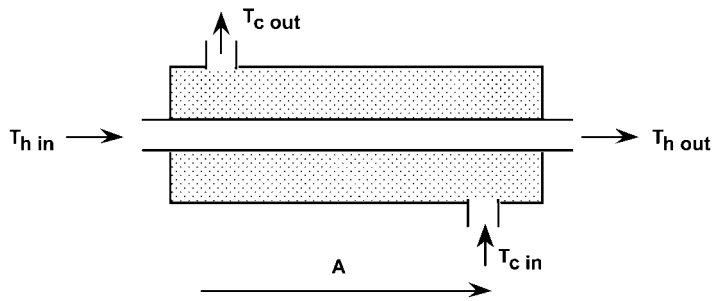

Fig. 4.26 Steady-state, countercurrent flow heat exchange.

Thus for the hot fluid

$$(W c_p)_h \Delta T_h = -U(T_h - T_c)\Delta A$$

and for the countercurrent cold fluid

$$(W c_p)_c \Delta T_c = -U(T_h - T_c)\Delta A$$

In the limit, the defining model equations for countercurrent flow become

$$\frac{dT_h}{dA} = -\frac{U(T_h - T_c)}{(Wc_p)_h}$$

and

$$\frac{dT_c}{dA} = -\frac{U(T_h - T_c)}{(Wc_p)_c}$$

where for cocurrent flow the sign in cold-fluid equation would be positive.

For design purposes the two equations can be integrated directly starting for the known temperature conditions at one end of the exchanger and integrating towards the known conditions at the other end, hence enabling the required heat exchange surface to be determined. This procedure is very similar to that of the steady-state mass transfer column calculation of Section 4.4.1.1. The design approach for a steady-state two-pass exchanger is illustrated by simulation example SSHEATEX.

However, the simulation of the steady-state performance for a heat exchanger with a known heat transfer surface area will demand an iterative split boundary solution approach, based on a guessed value of the temperature of one of the exit streams, as a starting point for the integration.

4.5.2.2 **Heat Exchanger Dynamics**

The modelling procedure is again based on that of Franks (1967). A simple, single-pass, countercurrent flow heat exchanger is considered. Heat losses and heat conduction along the metal wall are assumed to be negligible, but the dynamics of the wall (thick-walled metal tube) are significant.

Figure 4.27 shows the temperature changes over a small differential element of exchanger length ΔZ.

In this problem W is the mass flow rate (kg/s), T is temperature (K), c_p is the specific heat capacity (kJ/kg K), D is the diameter (m), U is the heat transfer coefficient (kJ/m^2 s K), Q is the rate of heat transfer (kJ/s), V is the volume (m^3), ρ is the density (kg/m^3) and A is the heat transfer area (m^2). The subscripts are as follows: t refers to tube conditions, s to shellside conditions, and m to the metal wall.

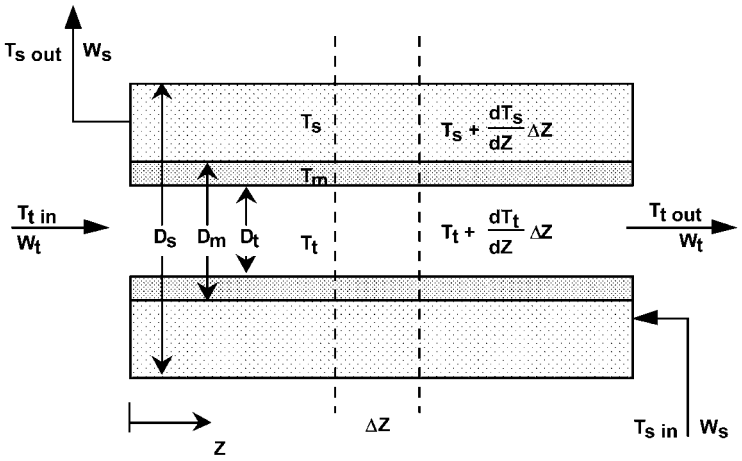

Fig. 4.27 Shell-and-tube heat exchanger: differential model.

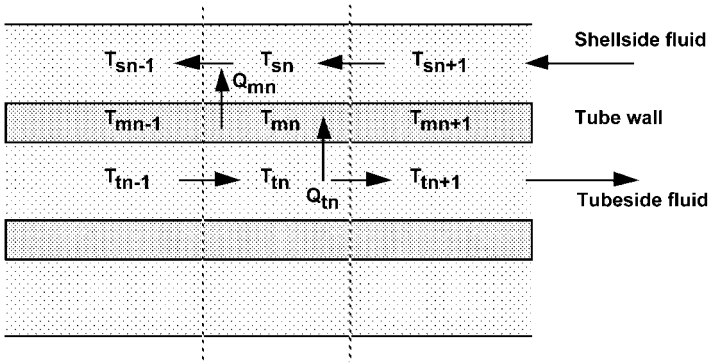

Fig. 4.28 Finite-differencing of heat exchanger length.

Heat balance equations on the element of heat exchanger length ΔZ according to enthalpy balance relationship

$$\begin{pmatrix}\text{Rate of}\\ \text{accumulation}\\ \text{of enthalpy}\\ \text{in the element}\end{pmatrix} = \begin{pmatrix}\text{Flow rate}\\ \text{of enthalpy}\\ \text{into}\\ \text{the element}\end{pmatrix} - \begin{pmatrix}\text{Flow rate}\\ \text{of enthalpy}\\ \text{out of}\\ \text{the element}\end{pmatrix} + \begin{pmatrix}\text{Rate of}\\ \text{heat transfer}\\ \text{to the element}\end{pmatrix}$$

lead to three coupled first-order partial differential equations, which can be converted into difference equations for simulation language solution using standard finite-difference formulae as mentioned in Section 4.6.

Alternatively, the difference-equation model form can be derived directly by dividing the length of the heat exchanger into N finite-difference elements or segments, each of length ΔZ, as shown in Fig. 4.28.

The heat balance equation can now be applied to segment n of the heat exchanger. The heat transfer rate equations are given by the following terms:

Rate of heat transfer from tube contents to the metal wall

$$Q_{tn} = U_t \Delta A_t (T_{tn} - T_{mn})$$

where U_t is the tubeside film heat transfer coefficient and ΔA_t is the incremental tubeside area

$$\Delta A_t = \pi D_t \Delta Z$$

Rate of heat transfer from the metal wall to the shellside contents

$$Q_{mn} = U_m \Delta A_m (T_{mn} - T_{sn})$$

where U_m is the film heat transfer coefficient from the wall to the shell and ΔA_m is the incremental metal wall outside area

$$\Delta A_m = \pi D_m \Delta Z$$

Using a similar treatment as described previously in Section 4.3.5, the resulting finite difference form of the enthalpy balance equations for any element n become

$$\frac{dT_n}{dt} = \frac{W_t c_{pt}}{2} \frac{(T_{tn-1} - T_{tn+1}) - Q_{tn}}{\Delta V_t c_{pt} \rho_t}$$

$$\frac{dT_{mn}}{dt} = \frac{(Q_{tn} - Q_{mn})}{\Delta V_m c_{pm} \rho_m}$$

$$\frac{dT_{sn}}{dt} = \frac{W_s c_{ps}}{2} \frac{(T_{sn+1} - T_{sn-1}) + Q_{mn}}{\Delta V_s c_{ps} \rho_s}$$

where

$$\Delta V_s = \frac{\Delta Z \pi (D_s^2 - D_m^2)}{4}$$

$$\Delta V_t = \frac{\Delta Z \pi D_t^2}{4}$$

$$\Delta V_m = \frac{\Delta Z \pi (D_m^2 - D_t^2)}{4}$$

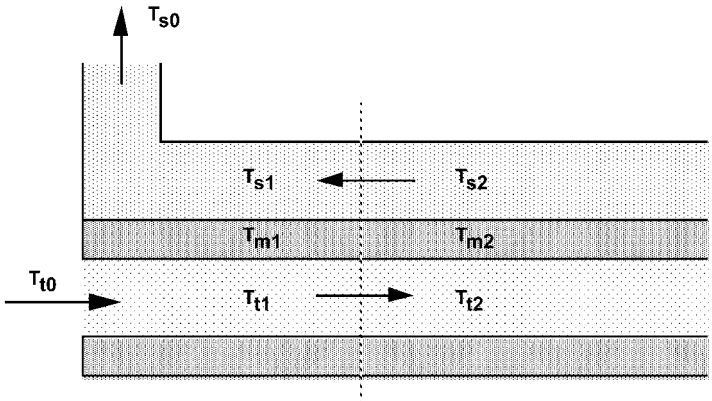

Fig. 4.29 Tube inlet and shell outlet segment.

Boundary Conditions

The consideration of the boundary conditions again follows Franks (1967). The position at the tube inlet and shell outlet section, segment number 1 is shown in Fig. 4.29.

Considering segment 1, the temperature of the entering shell side fluid is $(T_{s2}+T_{s1})/2$. The outlet shellside fluid temperature can also be approximated, either as

$$T_{s0} = T_{s1}$$

or

$$T_{s0} = T_{s1} + \frac{T_{s1} - T_{s2}}{2}$$

The heat balance equations for end segment 1 thus become

$$c_{ps}\rho_s \Delta V_s \frac{dT_{s1}}{dt} = W_s\, c_{ps}\left(\frac{T_{s2} + T_{s1}}{2} - T_{s0}\right) + Q_{m1}$$

and

$$c_{pt}\rho_t \Delta V_t \frac{dT_{t1}}{dt} = W_t\, c_{pt}\left(T_{t0} - \frac{T_{t1} + T_{t2}}{2}\right) - Q_{t1}$$

Similar reasoning for the tube outlet and shell inlet segment, number N, give for the tubeside fluid

$$\Delta V_t c_{pt}\rho_t \frac{dT_{tN}}{dt} = W_t c_{pt}\left(\frac{T_{tN-1} - T_{tN}}{2} - T_{tN+1}\right) - Q_{tN}$$

and for the shellside fluid

$$\Delta V_s c_{ps} \rho_s \frac{dT_{sN}}{dt} = W_s c_{ps} \left(T_{sN+1} - \frac{T_{sN} - T_{sN-1}}{2} \right) + Q_{mN}$$

Note that the outlet approximations must be consistent with a final steady-state heat balance. Note also that it is easy to allow in the simulation for variations in the heat transfer coefficient, density and specific heats as a function of temperature. The modelling methods demonstrated in this section are applied in the simulation example HEATEX.

4.6 Difference Formulae for Partial Differential Equations

As shown in this chapter for the simulation of systems described by partial differential equations, the differential terms involving variations with respect to length are replaced by their finite-differenced equivalents. These finite-differenced forms of the model equations are shown to evolve as a natural consequence of the balance equations, according to Franks (1967), and as derived for the various examples in this book. The approximation of the gradients involved may be improved, if necessary, by using higher order approximations. Forward and end-sections can be better approximated by the forward and backward differences as derived in the previous examples. The various forms of approximation based on the use of central, forward and backward differences have been listed by Chu (1969).

a) First-Order Approximations

Central difference as extensively used in this chapter

$$\left(\frac{\partial U}{\partial X} \right)_n = \frac{U_{n+1} - U_{n-1}}{2\Delta X}$$

$$\left(\frac{\partial^2 U}{\partial X^2} \right)_n = \frac{U_{n+1} - 2U_n + U_{n-1}}{\Delta X^2}$$

Forward difference

$$\left(\frac{\partial U}{\partial X} \right)_n = \frac{U_{n+1} - U_n}{\Delta X}$$

$$\left(\frac{\partial^2 U}{\partial X^2} \right)_n = \frac{U_{n+2} - 2U_{n+1} + U_n}{\Delta X^2}$$

Backward difference

$$\left(\frac{\partial U}{\partial X}\right)_n = \frac{U_n - U_{n-1}}{\Delta X}$$

$$\left(\frac{\partial^2 U}{\partial X^2}\right)_n = \frac{U_n - 2U_{n-1} + U_{n-2}}{\Delta X^2}$$

b) Second-Order Central Difference Approximations

$$\left(\frac{\partial U}{\partial X}\right)_n = \frac{-U_{n+2} + 8U_{n+1} - 8U_{n-1} + U_{n-2}}{12\Delta X}$$

$$\left(\frac{\partial^2 U}{\partial X^2}\right)_n = \frac{-U_{n+2} + 16U_{n+1} - 30U_n + 16U_{n-1} - U_{n-2}}{12\Delta X^2}$$

4.7 References Cited in Chapters 1 to 4

Aris, R. (1989) Elementary Chemical Reactor Analysis, Butterworth Publ., Stoneham.

Bird, R. B., Stewart, W. E. and Lightfoot, E. N. (1960) Transport Phenomena, Wiley.

Biwer, A., Heinzle, E. (2004) Environmental Assessment in Early Process Development. J. Chem. Technol. Biotechnol. 79, 597–609.

Blanch, H. W. and Clark, D. S. (1996) Biochemical Engineering, Marcel Dekker, New York.

Brodkey, R. S. and Hershey, H. C. (1988) Transport Phenomena, McGraw-Hill.

Carslaw, H. S. and Jaeger, J. C. (1959) Conduction of Heat in Solids, Clarendon Press.

Chu, Y. (1969) Digital Simulation of Continuous Systems, McGraw-Hill.

Coughanowr, D. R. and Koppel, L. B. (1965) Process Systems Analysis and Control, McGraw-Hill.

Dunn, I. J., Heinzle, E., Ingham, J. and Prenosil, J. E. (2003) Biological Reaction Engineering: Principles, Applications and Modelling with PC Simulation, 2nd edition, VCH.

Dunn, I. J. and Mor, J. R. (1975) Variable Volume Continuous Cultivation. Biotechnol. Bioeng. 17, 1805–1822.

Draper, N. R. and Smith, H. (1981) Applied Regression Analysis, Wiley.

Fogler, H. S. (2005) Elements of Chemical Reaction Engineering, 4th edition, Prentice-Hall.

Franks, R. G. E. (1967) Mathematical Modeling in Chemical Engineering, Wiley.

Franks, R. G. E. (1972) Modelling and Simulation in Chemical Engineering, Wiley-Interscience.

Froment, G. F. and Bischoff, K. B. (1990) Chemical Reactor Analysis and Design, Wiley.

Grewer, T. (1994) Thermal Hazards of Chemical Reactions, Elsevier Science.

Heinzle, E., Biwer, A. P. and Cooney, C. L. (2007) Development of Sustainable Bioprocesses – Modelling and Assessment, Wiley.

Heinzle, E. and Hungerbühler, K. (1997) Integrated Process Development: The Key to Future Production of Chemicals, Chimia, 51, 176–183.

Heinzle, E., Weirich, D., Brogli, F., Hoffmann, V., Koller, G., Verduyn, M. A. and Hungerbühler, K. (1998) Ecological and Economic Objective Functions for Screening in Integrated Development of Fine Chemical Processes. 1. Flexible and Expandable Framework Using

Indices. Ind. Eng. Chem. Res. 37, 3395–3407.
Ingham, J. and Dunn, I. J. (1974) Digital Simulation of Stagewise Processes with Backmixing. The Chem. Eng., June, 354–365.
Joshi, J. B., Pandit, A. B. and Sharma, M. M. (1982) Mechanically Agitated Gas-Liquid Reactors. Chem. Eng. Sci. 37, 813.
Kapur, J. N. (1988) Mathematical Modelling, Wiley.
Keller, A., Stark, D., Fierz, H., Heinzle, E. and Hungerbühler, K. (1997) Estimation of the Time to Maximum Rate Using Dynamic DSC Experiments. J. Loss Prev. Process Ind. 10, 31–41.
Keller, R. and Dunn, I. J. (1978) Computer Simulation of the Biomass Production Rate of Cyclic Fed Batch Continuous Culture. J. Appl. Chem. Biotechnol. 28, 508–514.
Koller, G., Weirich, D., Brogli, F., Heinzle, E., Hoffmann, V., Verduyn, M. A. and Hungerbühler, K. (1998) Ecological and Economic Objective Functions for Screening in Integrated Development of Fine Chemical Processes. 2. Stream Allocation and Case Studies. Ind. Eng. Chem. Res. 37, 3408–3413.
Levenspiel, O. (1999) Chemical Reaction Engineering, Wiley.
Luyben, M. L. and Luyben, W. L. (1997) Essentials of Process Control, McGraw-Hill.
Luyben, W. L. (1973) Process Modeling, Simulation, and Control for Chemical Engineers, McGraw-Hill
Luyben, W. L. (1990) Process Modelling, Simulation, and Control for Chemical Engineers, 2nd edition, McGraw-Hill.
Maria, G. and Heinzle, E. (1998) Kinetic System Identification by Using Short-Cut Techniques in Early Safety Assessment of Chemical Processes, J. Loss Prev. Process Ind. 11, 187–206.
Moser, A. (1988) Bioprocess Technology: Kinetics and Reactors, Springer.
Nash, J. C. and Walker-Smith, M. (1987) Nonlinear Parameter Estimation: An Integrated System in Basic, Marcel Dekker.
Noye, J. Ed. (1984) Computational Techniques for Differential Equations, North-Holland.
Oosterhuis, N. M. G. (1984) PhD Thesis, Delft University, The Netherlands.
Perlmutter, D. D. (1972) Stability of Chemical Reactors, Prentice-Hall.
Pollard, A. (1978) Process Control, Heinemann Educational Books.
Prenosil, J. E. (1976) Multicomponent Steam Distillation: A Comparison between Digital Simulation and Experiment. Chem. Eng. J. 12, 59–68.
Press, W. H., Flannery, B. P., Teukolsky, S. A. and Vetterling, W. T. (1992) Numerical Recipes: The Art of Scientific Computing, Cambridge University.
Ramirez, W. F. (1976) Process Simulation, Lexington Books.
Ruthven, D. M. and Ching, C. B. (1993) Modeling of chromatographic processes. Preparative and production scale chromatography. In: Chromatographic Science Series, Vol. 61. Eds. Ganetos, G., Barker, P. E. Marcel Dekker, pp. 629–672.
Seborg, D. E., Edgar, T. F., Mellichamp, D. A. (1989) Process Dynamics and Control, Wiley.
Shaw, J. A., The PID Control Algorithm: How It Works and How To Tune It., 2nd edition, eBook, Process Control Solutions (www.jashaw.com).
Sheldon, R. A. (1994) Consider the environmental quotient. Chem. Tech. 24/3, 38–47.
Shinskey, F. G. (1996) Process Control Systems: Application, Design, and Tuning 4th edition, McGraw-Hill.
Smith, C. L., Pike, R. W. and Murrill, P. W. (1970) Formulation and Optimisation of Mathematical Models, Intext.
Smith, R. (1995) Chemical Process Design, McGraw-Hill
Stephanopoulos, G. (1984) Chemical Process Control, Prentice-Hall.
Stoessel, F. (1995) Design thermally safe semibatch reactors. Chem. Eng. Prog. 9, 46–53.
Storti, G., Masi, M., Morbidelli, M. (1993) Modeling of countercurrent adsorption processes. Preparative and production scale chromatography. In: Chromatographic Science Series, Vol. 61. Eds. Ganetos, G., Barker, P. E. Marcel Dekker, New York, 673–700.
Strube, J., Schmidt-Traub, H., Schulte, M. (1998) Chem.-Ing.-Tech. 70, 1271–1279.

Sweere, A. P. J., Luyben, K. Ch. A. M. and Kossen, N. W. F. (1987) Regime Analysis and Scale-Down: Tools to Investigate the Performance of Bioreactors. Enzyme Microb. Technol., 9, 386–398.
Ullmann's Encyclopedia of Industrial Chemistry (1995) Production-integrated environmental protection, B8, 213–309, VCH.
Walas, S. M. (1989) Reaction Kinetics for Chemical Engineers, McGraw-Hill, reprinted by Butterworths.
Walas, S. M. (1991) Modelling with Differential Equations in Chemical Engineering, Butterworth-Heinemann Series in Chemical Engineering.
Welty, J. R., Wicks, C. E. and Wilson, R. E. (1976) Fundamentals of Momentum, Heat and Mass Transfer, Wiley.
Wilkinson, W. L. and Ingham, J. (1983) In: Handbook of Solvent Extraction, Eds. Lo, T. C., Baird, M. H. I., and Hanson, C., Wiley, pp. 853–886.

4.8 Additional Books Recommended

Al-Khafaji, A. W. and Tooley, J. R. (1986) Numerical Methods in Engineering Practice, Holt-Rinehart-Winston.
Aris, R. (1978) Mathematical Modelling Techniques, Pitman.
Aris, R. and Varma A. (1980) The Mathematical Understanding of Chemical Engineering Systems: Collected Papers of Neal R. Amundson, Pergamon.
Aris, R. (1999) Mathematical Modeling A Chemical Engineer's Perspective, Academic Press.
Babatunde, A., Ogunnaike, W., Harmon Ray (1994) Process Dynamics, Modelling and Control, Oxford University Press.
Beltrami, E. (1987) Mathematics for Dynamic Modelling, Academic Press.
Bender, E. A. (1978) An Introduction to Mathematical Modelling, Wiley-Interscience.
Bequette, B. W. (1998) Process Dynamics: Modeling, Analysis and Simulation, Prentice Hall.
Bequette, B. W. (2003) Process Control: Modeling, Design and Simulation, Prentice Hall.
Bronson, R. (1989) 2500 Solved Problems in Differential Equations, McGraw-Hill.
Burghes, D. N. and Borris, M. S. (1981) Modelling with Differential Equations, Ellis Horwood.
Butt, J. B. (2000) Reaction Kinetics and Reactor Design (Chemical Industries), Marcel Dekker.
Carberry, J. J. (1976) Chemical and Catalytic Reaction Engineering, McGraw-Hill.
Carberry, J. J. and Varma, A. (Eds.) (1987) Chemical Reaction and Reactor Engineering, Marcel Dekker.
Champion, E. R. and Ensminger, J. M. (1988) Finite Element Analysis with Personal Computers, Marcel Dekker.
Chapra, S. C. and Canale, R. P. (1988) Numerical Methods for Engineers, McGraw-Hill.
Constantinides, A. (1987) Applied Numerical Methods with Personal Computers, McGraw-Hill.
Courriou, J.-P. (2004) Process Control, Springer.
Cross, M. and Mascardini, A. O. (1985) Learning the Art of Mathematical Modelling, Ellis Horwood.
Darby, R. (2001) Chemical Engineering Fluid Mechanics, CRC Press.
Davis, M. E. (1984) Numerical Methods and Modeling for Chemical Engineers, Wiley.
Denn, M. M. (1987) Process Modelling, Longman Scientific and Technical Publishers.
Douglas, J. M. (1972) Process Dynamics and Control, Vols. 1 and 2, Prentice Hall.
Douglas, J. M. (1988) Conceptual Design of Chemical Processes, McGraw-Hill.
Finlayson, B. A. (1980) Nonlinear Analysis in Chemical Engineering, McGraw-Hill.
Fishwick, P. A. and Luker, P. A. (Eds.) (1991) Qualitative Simulation, Modelling and Analysis, Springer.
Gates, B. C. (1992) Catalytic Chemistry, Wiley.

Geankoplis, C. J. (1983) Transport Processes and Unit Operations, 2nd edition, Allyn and Baker.
Guenther, R. B. and Lee, J. W. (1988) Partial Differential Equations of Mathematical Physics and Integral Equations, Prentice-Hall.
Hannon, B. and Ruth, M. (1994) Dynamic Modeling, Springer.
Hayes, R. E. (2001) Introduction to Chemical Reactor Analysis, Gordon and Breach Science Publishers.
Himmelblau, D. M. (1985) Mathematical Modelling. In: Bisio, E. and Kabel, R. L. (Eds.) Scaleup of Chemical Processes, Wiley.
Hines, A. L. and Maddox, R. N. (1985) Mass Transfer, Prentice-Hall.
Holland, C. D. and Anthony, R. G. (1989) Fundamentals of Chemical Reaction Engineering, 2nd edition, Prentice-Hall.
Holland, C. D. and Liapis, A. I. (1983) Computer Methods for Solving Dynamic Separation Problems, McGraw-Hill.
Huntley, I. D. and Johnson, R. M. (1983) Linear and Nonlinear Differential Equations, Ellis Horwood.
Hussam, A. (1986) Chemical Process Simulation, Halstead/Wiley.
Kaddour, N. (Ed.) (1993) Process Modeling and Control in Chemical Engineering, Marcel Dekker.
Kocak, H. (1989) Differential and Difference Equations Through Computer Experiments, with Diskette, Springer.
Korn, G. A. and Wait, J. V. (1978) Digital Continuous System Simulation, Prentice Hall.
Lapidus, L. and Pinder, G. F. (1982) Numerical Solution of Partial Differential Equations in Science and Engineering, Wiley-Interscience.
Leesley, M. E. (Ed.) (1982) Computer Aided Process Plant Design, Gulf Publishing Company.
Lo, T. C., Baird, M. H. I., and Hanson, C. (1983) Handbook of Solvent Extraction, Wiley.
Loney, N. W. (2001) Applied Mathematical Methods for Chemical Engineers, CRC Press.
Luyben, W. L. (2002) Plantwide Dynamic Simulators in Chemical Processing and Control, Marcel Dekker.
Marlin, T. E. (2000) Process Control: Designing Processes and Control Systems for Dynamic Performance, 2nd edition, McGraw-Hill College.
Missen, R. W., Mims, C. A. and Saville, B. A. (1999) Introduction to Chemical Reaction Engineering and Kinetics, John Wiley & Sons, Inc.
Morbidelli, M and Varma, A. (1997) Mathematical Methods in Chemical Engineering, Oxford University Press.
Naumann, E. B. (1987) Chemical Reactor Design, Wiley.
Naumann, E. B. (1991) Introductory Systems Analysis for Process Engineers, Butterworth-Heinemann.
Naumann, E. B. (2001) Chemical Reactor Design, Optimization and Scaleup, McGraw-Hill.
Neelamkavil, F. (1987) Computer Simulation and Modelling, Wiley.
Ogunnaike, B. A. and Ray, W. H. (1994) Process Dynamics, Modeling, and Control, Oxford Univ. Press.
Palazoglu, A. and Romagnoli, J. A. (2005) Introduction To Process Control, Marcel Dekker.
Peters, M. S., Timmerhaus, K. D., and West, R. E. (2003) Plant Design and Economics for Chemical Engineers, 5th edition, McGraw-Hill.
Ramirez, W. F. (1989) Computational Methods for Process Simulation, Butterworth-Heinemann.
Rase, H. F. (1977) Chemical Reactor Design for Process Plants, Vol. 11: Case Studies and Design Data, Wiley.
Richardson, J. F. and Peacock, D. G. (1994) Coulson & Richardson's Chemical Engineering, Vol. 3: Chemical & Biochemical Reactors & Process Control, Pergamon.
Riggs, J. B. (1988) An Introduction to Numerical Methods for Chemical Engineers, Texas Techn. Univ. Press.
Robinson, E. R. (1975) Time-Dependent Chemical Processes, Applied Science.
Russell, T. W. F. and Denn, M. M. (1972) Introduction to Chemical Engineering Analysis, Wiley.
Seider, W. D., Seader, J. D., Lewin, D. R. (2004) Product and Process Design Principles, Synthesis, Analysis, and Evaluation, 2nd edition, Wiley.

Schmidt, L. D. (1998) The Engineering of Chemical Reactions, Oxford Univ. Press.
Shuler, M. L.and Kargi, F. (2002) Bioprocess Engineering. Basic Concepts; Prentice Hall: USA
Smith, C. A. and Corripio, A. B. (1985) Principles and Practice of Automatic Process Control, Wiley.
Smith, J. M. (1981) Chemical Engineering Kinetics, McGraw-Hill.
Smith, J. M. (1987) Mathematical Modelling and Digital Simulation for Engineers and Scientists 2nd edition, Wiley-Interscience.
Stewart, W. E., Ray, W. H. and Conley, C. C. (1980) Dynamics and Modeling of Reactive Systems, Academic Press.
Szekely, J. and Themelis, N. J. (1971) Rate Phenomena in Process Metallurgy, Wiley.
Tarhan, M. O. (1983) Catalytic Reactor Design, McGraw-Hill.
Turton, R., Baillie, R. C., Whiting, W. B. and Shaeiwitz, J. A. (2002) Analysis, Synthesis, and Design of Chemical Processes, 2nd edition, Prentice Hall.
Ulrich, G. D. and Vasudevan, P. T. (2004) Chemical Engineering Process Design and Economics: A Practical Guide, 2nd edition, Process Publishing, Durham.
Vemuri, V. and Karplus, W. J. (1981) Digital Computer Treatment of Partial Differential Equations, Prentice-Hall.
Wankat, P. C. (1990) Rate Controlled Separations, Elsevier Applied Science.
Woods, D. R. (1995) Process Design and Engineering Practice, Prentice-Hall.
Zwillinger, D. (1989) Handbook of Differential Equations, Academic Press.